Technical Report Documentation Page

1. Report No.	2. Government Accession No.	3. Recipient's Catalog No.
UM-HSRI-78-4		

4. Title and Subtitle	5. Report Date
DEVELOPMENT OF TECHNIQUES FOR INVESTIGATING ACCIDENT CAUSATION	1/78
	6. Performing Organization Code
7. Author(s)	8. Performing Organization Report No.
Leonard Johnson and Leonard Segel	UM-HSRI-78-4
9. Performing Organization Name and Address	10. Work Unit No.
Highway Safety Research Institute The University of Michigan Huron Parkway and Baxter Road Ann Arbor, Michigan 48109	11. Contract or Grant No. 361283
	13. Type of Report and Period Covered 7/1/76 - 12/31/77 Final
12. Sponsoring Agency Name and Address Motor Vehicle Manufacturers Association 320 New Center Building Detroit, Michigan 48202	14. Sponsoring Agency Code MVMA Project 4.29

15. Supplementary Notes

16. Abstract

Distributions of understeer coefficients and steering sensitivities are computed for (1) an OE vehicle population, (2) an at-risk vehicle population, and (3) an accident-involved vehicle population to determine if these vehicle handling parameters could be influential in accident causation. The influences of in-use tire factors (inflation pressure and tread depth) and in-use loading conditions (as reflected by number of occupants) upon understeer and steering sensitivity are reflected in the distributions calculated for the at-risk and accident-involved populations.

It is concluded that no differences of any consequence exist between the distributions of either understeer or steering sensitivity as calculated for the at-risk and accident-involved vehicle populations. This conclusion is qualified by the following points: (1) knowledge of the effects of inflation pressure and tread depth on tire stiffness properties is imprecise, (2) the effects of mixing of tire sizes and constructions on understeer and steering sensitivity in the at-risk population is ignored, and (3) the sample of accident vehicles is somewhat small (a total of 218 vehicles).

17. Key Words	18. Distribution Statement
understeer, steering sensitivity, OE vehicle population, at-risk vehicle population, accident-involved vehicle population, in-use tire factors, in-use vehicle loading	UNLIMITED

19. Security Classif. (of this report)	20. Security Classif. (of this page)	21. No. of Pages	22. Price
NONE	NONE	85	

UM-HSRI-78-4

DEVELOPMENT OF TECHNIQUES FOR INVESTIGATING ACCIDENT CAUSATION

Final Report

MVMA Project No. 4.29

Leonard Johnson
Leonard Segel

January 1978

Sponsored by

The Motor Vehicle Manufacturers Association

TABLE OF CONTENTS

ACKNOWLEDGEMENTS

The authors wish to express their appreciation of the efforts of the following people who also contributed to this study.

Graduate Assistants Howard Moncarz and Jack Brown compiled the large amount of data which made up the library of tire stiffness data, and also developed the procedures to correct tire stiffness data for the effects of inflation pressure and tread depth.

Mr. Peter VanEck spent many, many hours gleaning data from the MVMA passenger car specification sheets and coding it for use in a computer file.

Our liaison with the Systems Analysis Division of HSRI was Mr. Bob Scott, who provided us with much data maintained by Systems Analysis, and who was always interested in the findings of the project as they developed.

Special thanks must go to Ms. Jeannette Nafe for her excellent work of typing this report.

1.0 INTRODUCTION

Trying to assess the role of vehicle handling in accident causation has been and still is a very difficult task. Many factors, such as driver competence, road conditions, and traffic conditions, to name a few, interact in the accident process. Thus, the role of vehicle handling performance is highly obscured. Dunlap, et al., have addressed this problem at some length [1].

It is well known that handling characteristics of vehicles can be altered by tire in-use factors. Departures of inflation pressure from recommended values, tread depth differentials, improper replacements of tires, and extreme values of wheel loading can combine to significantly change the handling properties originally designed into a vehicle. It can be hypothesized that if vehicle handling does play a significant role in accident causation, then certain vehicle handling parameters should differ for the at-risk population and the accident-involved population. In particular, it would be of interest to compare understeer and steering sensitivity (as determined by in-use tire factors) for the two vehicle populations of interest.

This project is a study of the feasibility of making such comparisons. Calculations are made of the distributions of understeer coefficients and steering sensitivities (i.e., lateral acceleration per unit steering wheel angle) for the at-risk population of domestic vehicles in Washtenaw and Oakland Counties and a sample of accident-involved vehicles in these same counties.* In-use tire and loading factors are assumed to have the major influence on these two vehicle handling performance measures.

The report begins with a statement of the objectives of the study, followed by an overall description of the methodology that

---

*These populations were restricted to 1972-1976 model year domestic passenger cars.

was employed. After presenting the findings that were obtained, a number of conclusions are drawn and recommendations for further work are made. Various details of the methodology and its implementation using specially designed computer codes are documented in six appendices.

2.0 OBJECTIVES

The objective of this project was to determine the feasibility of estimating steering response characteristics for both individual vehicles and entire vehicle populations as they are affected by in-use tire and loading conditions. Provided feasibility was demonstrated, a second objective was to calculate the distribution of these response characteristics for an at-risk vehicle population and an accident-involved vehicle population. In this manner, the role of vehicle handling in accident causation could be evaluated in terms of these particular characteristics.

3.0 METHODOLOGY

A procedure for estimating the understeer coefficient and steering sensitivity of an individual car constitutes the sine qua non of this study. Given that this estimation requires information that is either not available or is very difficult to obtain, it was necessary that the estimation procedure be reduced to its bare essentials. Accordingly, the expression for understeer coefficient, as derived and developed for the linear automobile by a number of investigators [2, 3, 4], was reduced to the following expression, on the basis of assumptions to be discussed below:

$$K = \frac{\left[W_F + (C_{\gamma_1} + C_{\gamma_2}) \frac{\partial \gamma_F}{\partial \phi} \frac{\partial \phi}{\partial a_y}\right]\left[1 + (N_{\alpha_1} + N_{\alpha_2}) \frac{\partial \psi}{\partial M_{zF}}\right]}{C_{\alpha_1} + C_{\alpha_2}} - \frac{W_R}{C_{\alpha_3} + C_{\alpha_4}} \quad \text{deg/g} \qquad (1)$$

where

$W_{F,R}$ = front,rear axle loads (lb)

$C_{\alpha_{1,2,3,4}}$ = LF, RF, LR, RR cornering stiffness (lb/deg)

$C_{\gamma_{1,2}}$ = LF, RF camber stiffness (lb/deg)

$N_{\alpha_{1,2}}$ = LF, RF aligning moment stiffness (ft-lb/deg)

$\frac{\partial \gamma_F}{\partial \phi}$ = roll camber rate of front suspension (deg/deg)

$\frac{\partial \phi}{\partial a_y}$ = roll compliance of vehicle (deg/g)

$\frac{\partial \psi}{\partial M_{zF}}$ = front aligning moment compliance steer (deg/ft-lb)

(It should be noted that all of these quantities are assumed to be positive. This practice differs from the SAE sign conventions for some of these quantities, but makes the calculation algebraically simpler.)

It will be noted that many of the design variables contributing to understeer do not appear in Equation (1). Specifically, the aligning moments acting on the overall vehicle have been ignored since their influence is very small. Suspension roll-steer properties have not been included because (1) these data are generally not available, (2) roll-steer effects are not influenced significantly by in-use variables, and (3) this property is almost always controlled by the designer to be small or to add to the understeer quality of the vehicle. In addition, the influence of suspension compliance effects has been neglected, with the exception of "front aligning moment compliance steer." Although the primary reason for neglecting suspension compliance effects is the absence of data, it is also true that these effects are small in comparison with the major factors influencing the understeer coefficient.

The influence of "front aligning moment compliance steer" on understeer is widely recognized, and measurements have been published for a number of vehicles. The aggregate net effect of all of the factors which have been neglected is an increase in understeer. Thus, calculations of the understeer coefficient using Equation (1) can be expected to be somewhat low.

Steering sensitivity was calculated using the following equation:

$$ss = \frac{1}{(\frac{g\ell}{V^2}\ \frac{180}{\pi} + K)GR} \quad g's/deg \qquad (2)$$

where

g = acceleration of gravity (fps^2)

ℓ = wheelbase (ft)

V = forward speed (fps)

GR = overall steering ratio

This performance numeric was calculated in this study for a speed of 40 mph (selected as representative of suburban driving conditions) and is expressed as g's/100 degrees of steering-wheel angle. Because the understeer coefficients estimated by Equation (1) are expected to be somewhat small, calculations of steering sensitivity can be expected to be somewhat large.

Tire stiffness data were obtained from tests performed on approximately 300 different tires by the Calspan Corporation [5]. Because these tests were performed at a cold inflation pressure of 24 psi and full tread depth, procedures were developed to correct these stiffness measurements to account for the in-use variables of inflation pressure and actual tread depth. Unfortunately, these corrections had to be based on minimal amounts of data. The manner in which the tire data are assembled and corrections are applied to these stiffness data are detailed in Appendix A.

A common value of roll camber rate was assumed to apply to all vehicles, namely, 0.90 deg/deg which is the median of the values to be found in the open literature. In addition, a fixed value of 0.54 deg/100 ft-lb was used for "front aligning moment compliance steer." This value was likewise the median of the data to be found in the literature.

The original plan to account for the influence of roll compliance was to use fixed values for different categories of vehicles; i.e., one value for vehicles in the sport category, another for family sedans, etc. However, an examination of the data available in the literature did not support this scheme. Accordingly, an estimation procedure for roll compliance was developed using certain chassis parameter data from the passenger car specification sheets that are prepared by the Motor Vehicle Manufacturers Association (MVMA). The roll compliance estimation and the selection of values for the roll camber rate and "front aligning moment compliance steer" are detailed in Appendix B.

To evaluate the accuracy of the adopted understeer estimation procedure, a comparison was made between measured and estimated

understeer coefficients for nine passenger cars. The results are shown in Table 1 and in Figure 1. As can be seen, the agreement between measured and estimated values of understeer is quite reasonable. On the whole, the estimated values are somewhat less than the measured values, as expected. It was concluded that the estimation procedure produces usable values of understeer coefficients.

Having demonstrated that it is feasible to estimate understeer by the developed computational procedure, understeer and steering sensitivity distributions can be calculated for the (1) OE vehicle population, (2) at-risk vehicle population, and (3) accident-involved population, provided the required data are available or can be developed.

Distributions of understeer and steering sensitivity were first calculated for the OE vehicle population. The necessary vehicle specifications (tire size, inflation pressure, axle loads, etc.) were compiled for each vehicle from the MVMA specification sheets. (The procedure for assembling the vehicle parameter data is outlined in Appendix C.) These computations were performed for each OE vehicle in the driver-only loading condition, yielding distributions of understeer coefficient and steering sensitivity which could then be expanded to account for the following in-use factors: (1) tire inflation pressure and tread depth, (2) vehicle loading (as determined by the number of occupants), and (3) the distribution of makes and models in the at-risk population.

The manner in which inflation pressure and tread depth, respectively, vary in an in-use population of vehicles was determined from data collected by the Systems Analysis Division of HSRI, in conjunction with a checklane operated by the Michigan State Police in Jackson County in July, 1976 [11]. The data were first scrutinized to investigate for dependencies of these factors on vehicle age, size, or type (i.e., station wagon or non-station wagon) (see Appendix D). Since it was determined that tread depth is dependent on vehicle age, the in-use tire data was divided into five groups according to vehicle age in years.

Table 1. Comparison of Measured and Predicted Values of Understeer.

Vehicle	Understeer Coefficient (deg/g) Measured	Predicted	Reference
1971 Ford Mustang	4.60	3.55	6
1973 Buick Century	6.09	4.86	6
1973 Chevrolet Caprice	4.93	5.22	7
1974 Chevrolet Nova	5.26	3.82	7
1969 Ford Galaxie	8.15	4.57	8
1970 Ford Torino	5.14	5.83	9
1970 Ford Torino	6.07	6.28	9
1970 Ford Torino	6.31	4.78	9
1973 Plymouth Fury	5.78	5.03	10

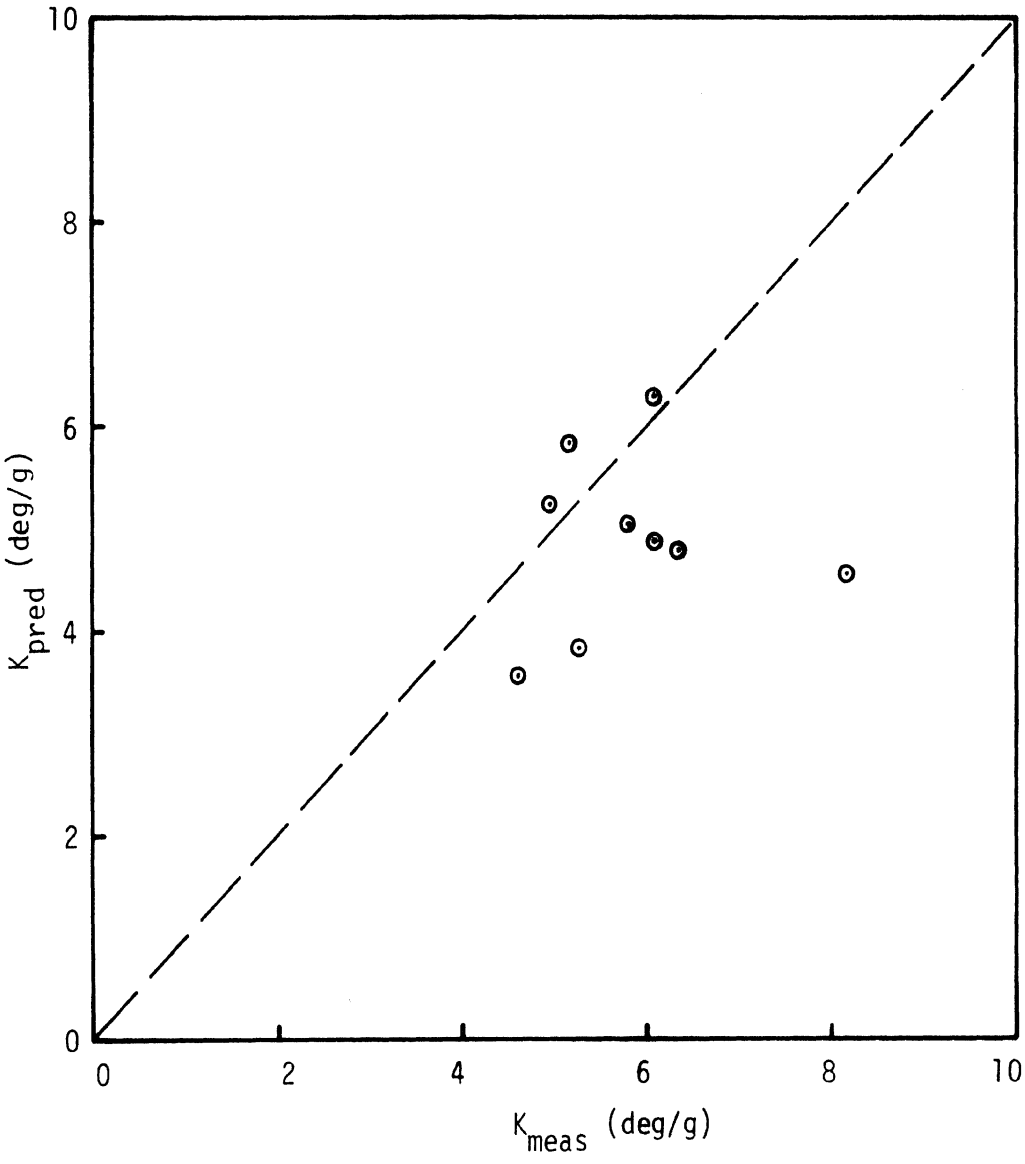

Figure 1. Predicted vs. measured values of understeer (dashed line indicates $K_{pred} = K_{meas}$).

To calculate the required distributions, the in-use tire factors were first applied to an OE vehicle to develop distributions for each loading condition (i.e., number of occupants equal to 1, 2, 3, etc.). For a given number of occupants in a particular vehicle, the inflation pressure and tread depth condition of each case vehicle from the appropriate age category of the checklane data was applied in succession. Thus, one value of understeer was calculated for each inflation pressure-tread depth combination from the checklane. Oftentimes, two steering sensitivity distributions were calculated for each loading condition because of the availability of two OE steering ratios (manual and power steering). These distributions were weighted by the power steering installation rate published in annual vehicle production summaries [12] and combined.

These separate distributions were then combined into one distribution which reflected the influence of loading, by weighting the individual distributions in accordance with data available defining the occupant probabilities (see Appendix D). An assumption is thus being made that tire-in-use factors are independent of the number of occupants. This assumption appears reasonable for short trips, but for long trips with full passenger loads (e.g., vacation travel) more attention may be paid to the condition of tires.

Finally, the distributions of understeer and steering sensitivity computed for each vehicle were combined in a manner that accounted for the distribution of makes and models in the at-risk population of interest; i.e., the vehicles registered in Washtenaw and Oakland Counties (see Appendix E). The at-risk population was localized in this manner because the data collected to calculate the distributions for accident-involved vehicles were, and are, being obtained from these same two counties.

The last task in the study requires the computation of the understeer and steering sensitivity of accident-involved vehicles. The necessary data (tire sizes, inflation pressures, tread depths, and occupant weights) were compiled from accident records maintained by Systems Analysis [13, 14]. (The manner in which this information was assembled is detailed in Appendix C.) Understeer and steering sensitivity were computed for each accident-involved vehicle using data

collected from the accident scene in conjunction with information gathered from the MVMA specification sheets. These calculations could then be assembled to yield a distribution of understeer and steering sensitivity as possessed by an accident-involved population of passenger cars.

A detailed description of the computational procedures used to develop the various distributions is given in Appendix F.

4.0 FINDINGS

Distributions of understeer and steering sensitivity, as estimated for the OE vehicle population, are shown in Figures 2a and b and 3a and b. It should be noted that these distributions have been calculated assuming two inflation pressure conditions: (1) recommended inflation pressures for maximum load and (2) 24 psi. The inflation pressures for maximum loads were used because these pressures are given in the MVMA specification sheets. Since, however, these calculations were performed for the driver-only loading condition, the appropriate inflation pressures would have been the pressures recommended for light loads. However, this information is not available and, accordingly, calculations were performed by assuming all tires to be inflated to 24 psi.

An examination of the results computed for the OE population yields the following findings:

- Inflation Pressures at Values Recommended for Maximum Load
  - Understeer coefficient
    - population size: 374
    - mean: 3.74 deg/g
    - standard deviation: 1.09 deg/g
  - Steering sensitivity
    - population size: 572
    - mean: 0.558 g's/100 deg
    - standard deviation: 0.147 g's/100 deg
- All Tires Inflated to 24 psi
  - Understeer coefficient
    - population size: 374
    - mean: 3.62 deg/g
    - standard deviation: 1.15 deg/g

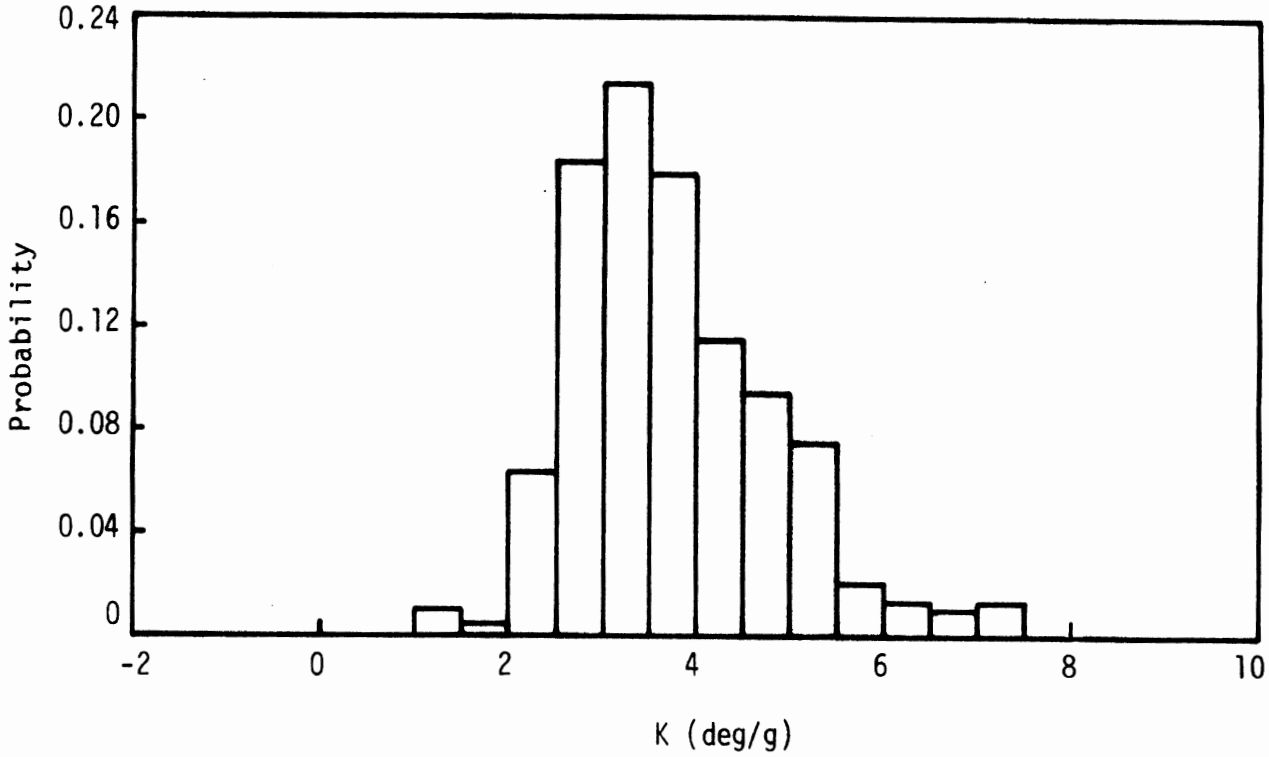

(a) Understeer

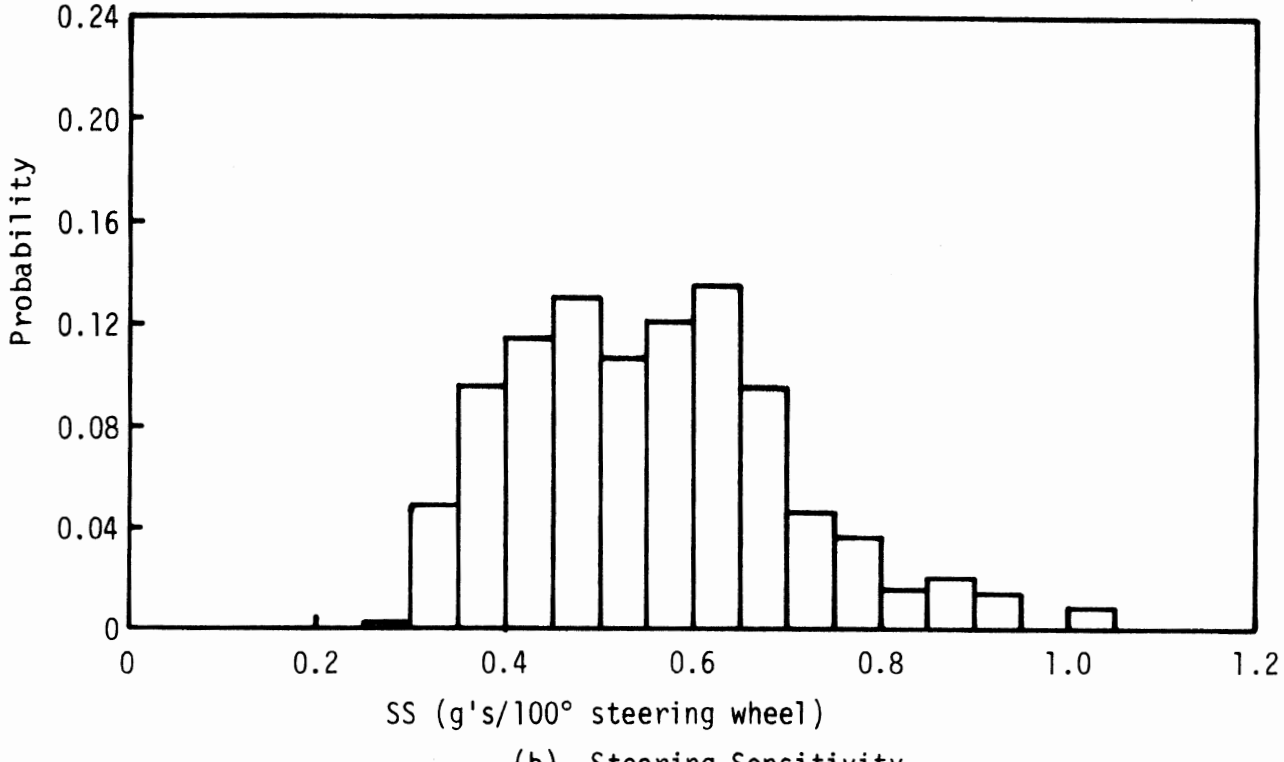

(b) Steering Sensitivity

Figure 2. Distributions of understeer and steering sensitivity for the OE vehicle population assuming all tires inflated to pressures recommended for maximum load conditions.

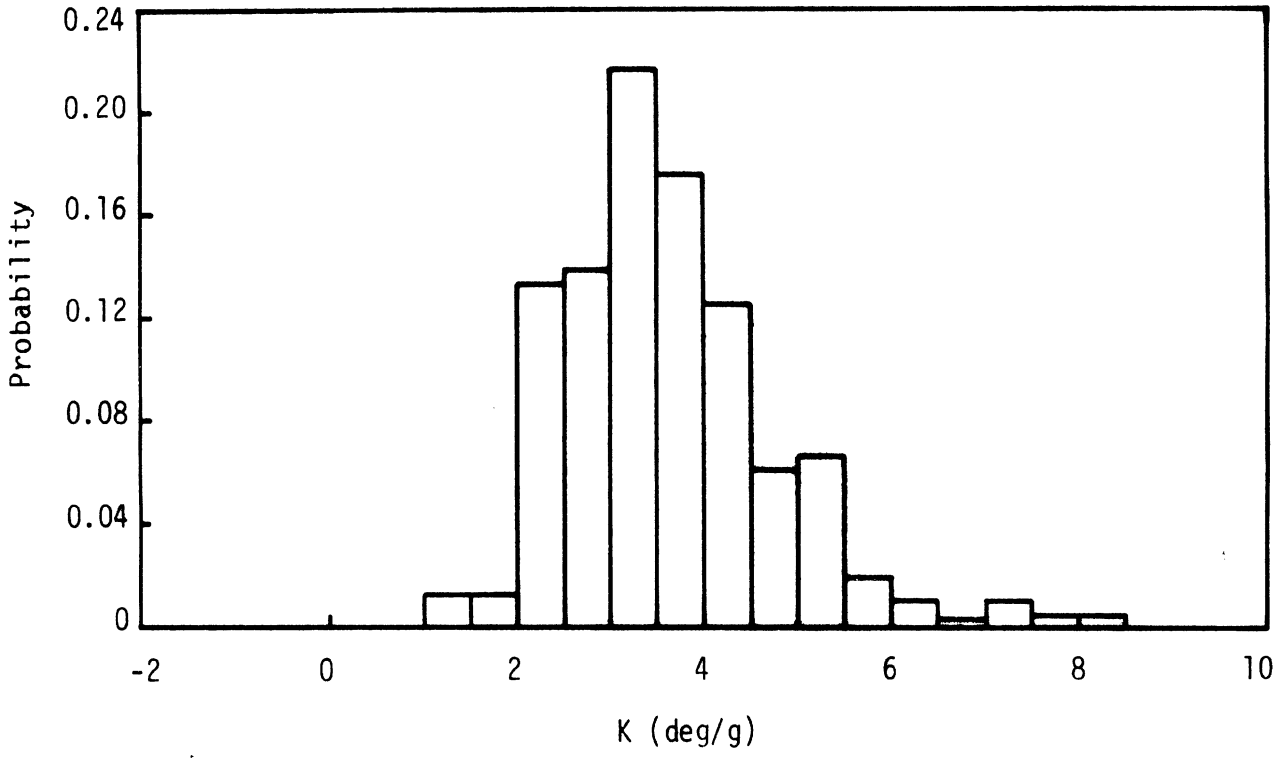

(a) Understeer

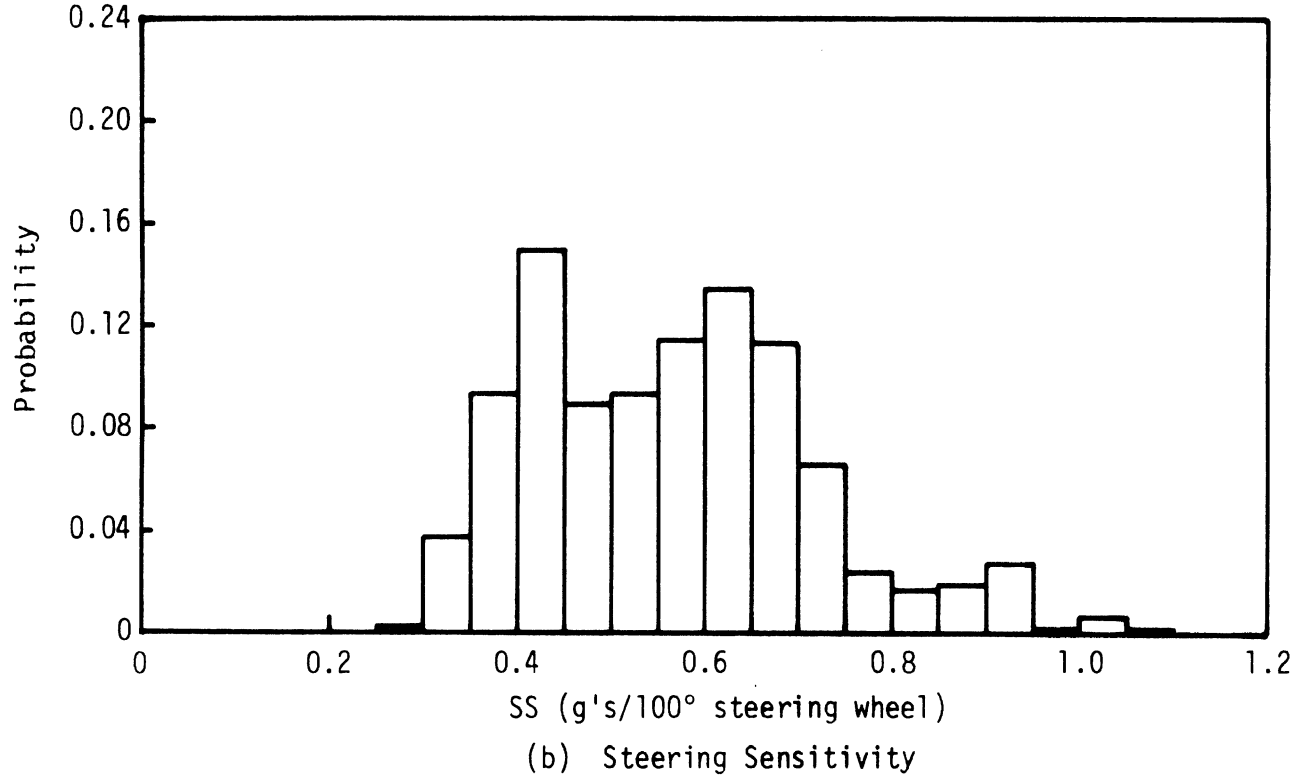

(b) Steering Sensitivity

Figure 3. Distributions of understeer and steering sensitivity for the OE vehicle population assuming all tires inflated to 24 psi.

- Steering sensitivity
  - population size: 572
  - mean: 0.567 g's/100 deg
  - standard deviation: 0.152 g's/100 deg

Note that the difference in sample size used to compute the distribution of understeer and steering sensitivity results from the availability of two steering ratios for many of the cars in the total population. It should also be noted that these OE calculations have been performed only for the so-called base vehicle, that is, the vehicle without options. It can be assumed that, as options are added to a vehicle and the weight of the vehicle is increased, changes in tire sizes (and suspensions) are made using the optional tire sizes called out in the MVMA specification sheets.

The distributions of understeer and steering sensitivity estimated for a typical vehicle of a given make, model, and model year, as derive from in-use distributions of inflation pressure, tread depth, and loading, are shown in Figures 4a and b. The mean value of understeer is 3.46 deg/g, slightly lower than the value of 3.58 deg/g that was obtained for the OE vehicle by assuming all tires to be inflated to 24 psi. The standard deviation is 0.47 deg/g. Approximately 90% of the distribution lies within ±40% of the mean. The mean value of the steering sensitivity is 0.667 g's/100 deg (at 40 mph), slightly larger than the 0.644 g's/100 deg calculated for the OE vehicle. The standard deviation is 0.053 g's/100 deg.

The distributions of understeer and steering sensitivity computed for the entire in-use vehicle population are shown in Figures 5a and b. The mean value of the understeer coefficient is 3.53 deg/g and the standard deviation is 1.61 deg/g. It is observed that the mean is slightly less than that calculated for the OE population, while the standard deviation is substantially greater. Approximately 90% of the distribution is found to lie between 1.5 and 6 deg/g. The mean value of steering sensitivity is 0.631 g's/100 deg (at 40 mph) and the standard deviation is 0.138 g's/100 deg. About 90% of the

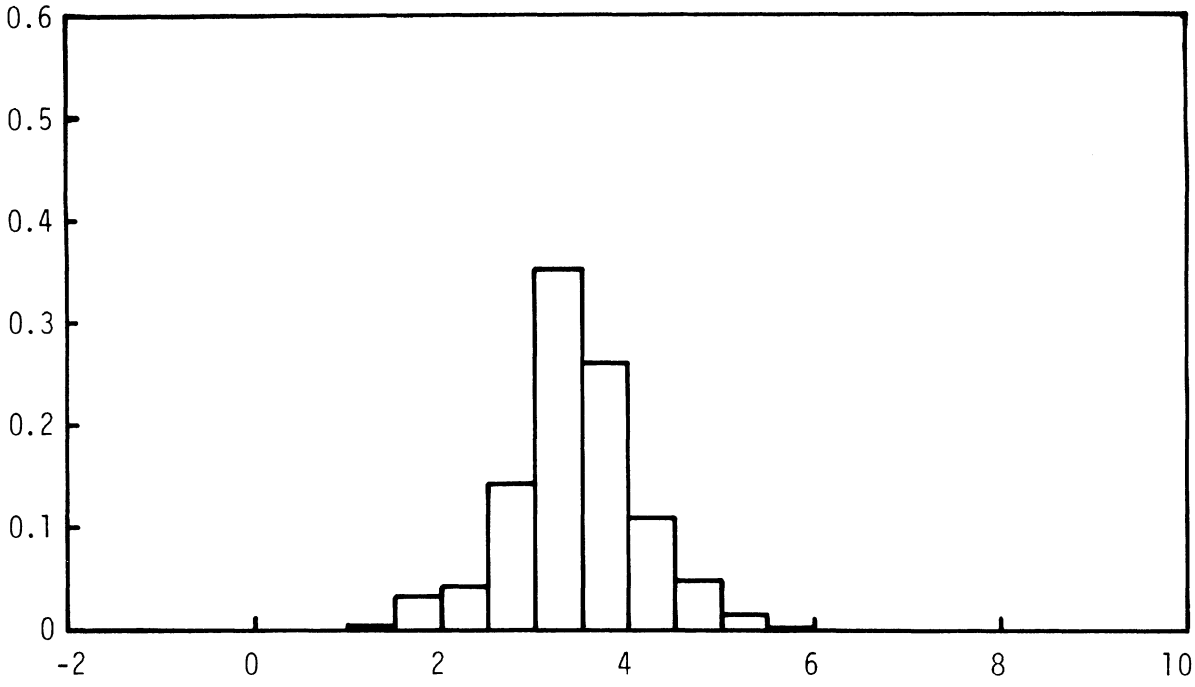

(a) Understeer

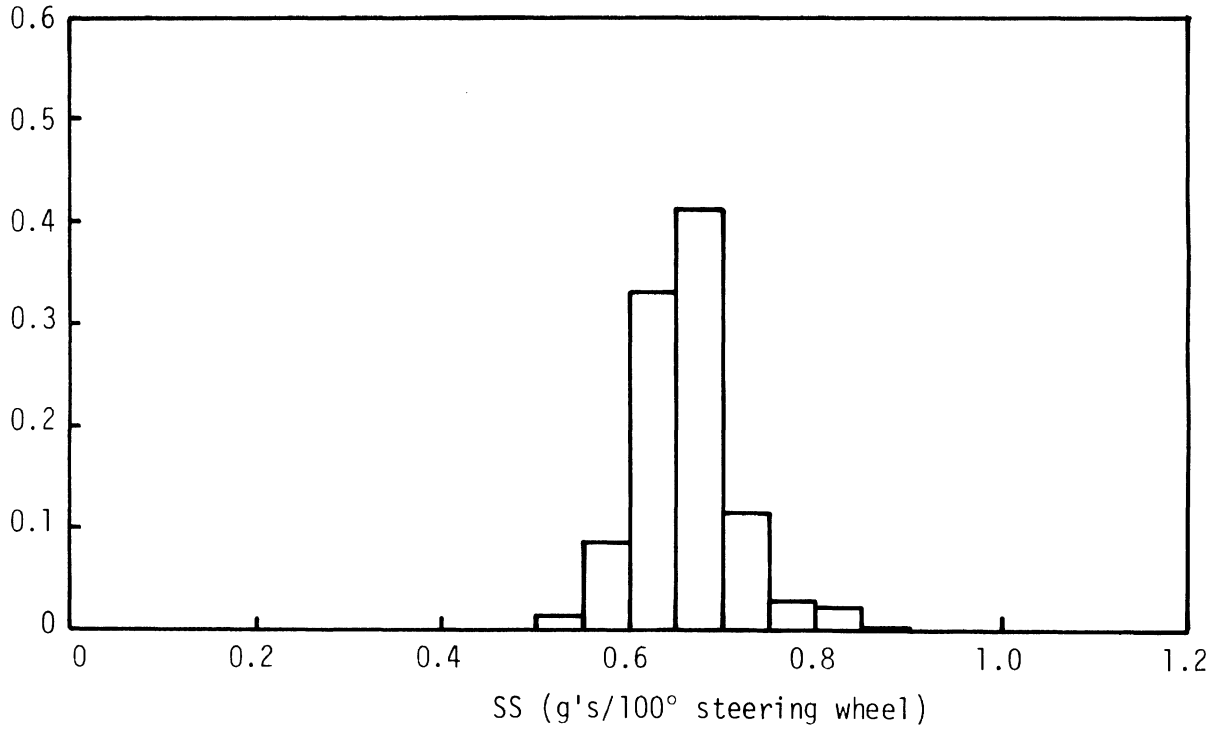

(b) Steering Sensitivity

Figure 4. Distributions of understeer and steering sensitivity for a typical vehicle of a given make, model, and model year from the at-risk population.

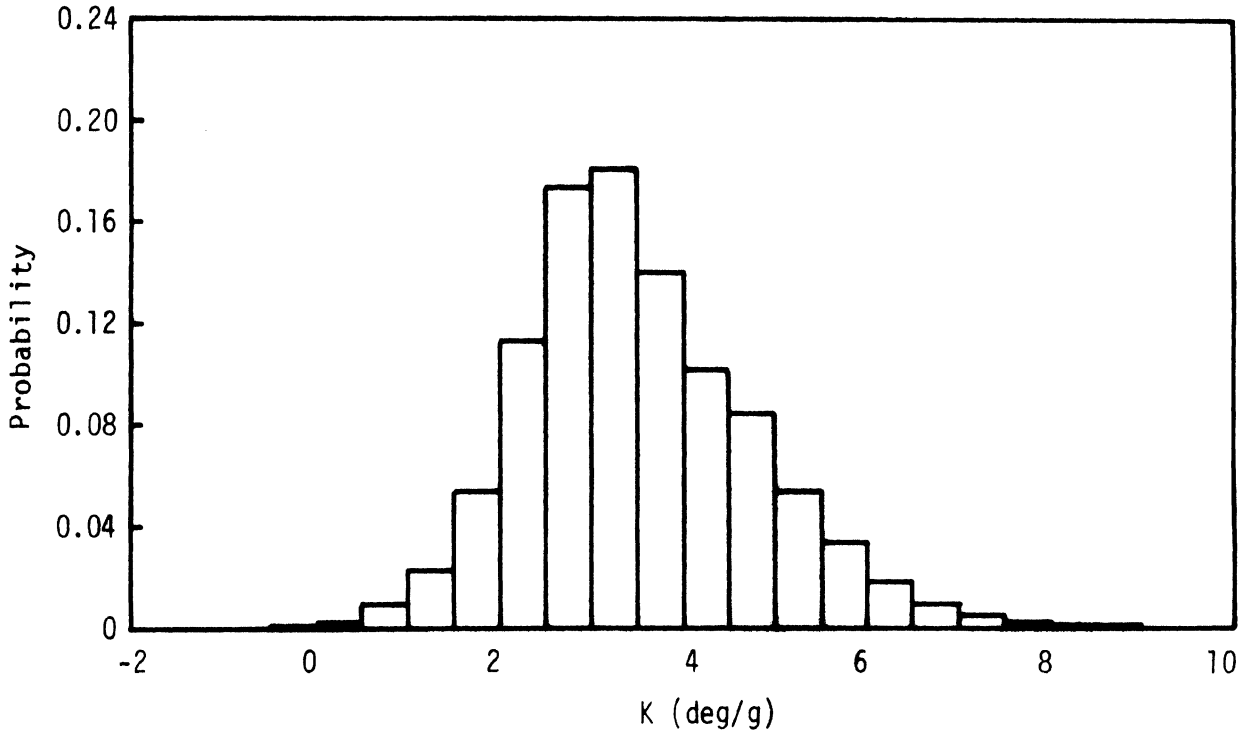

(a) Understeer

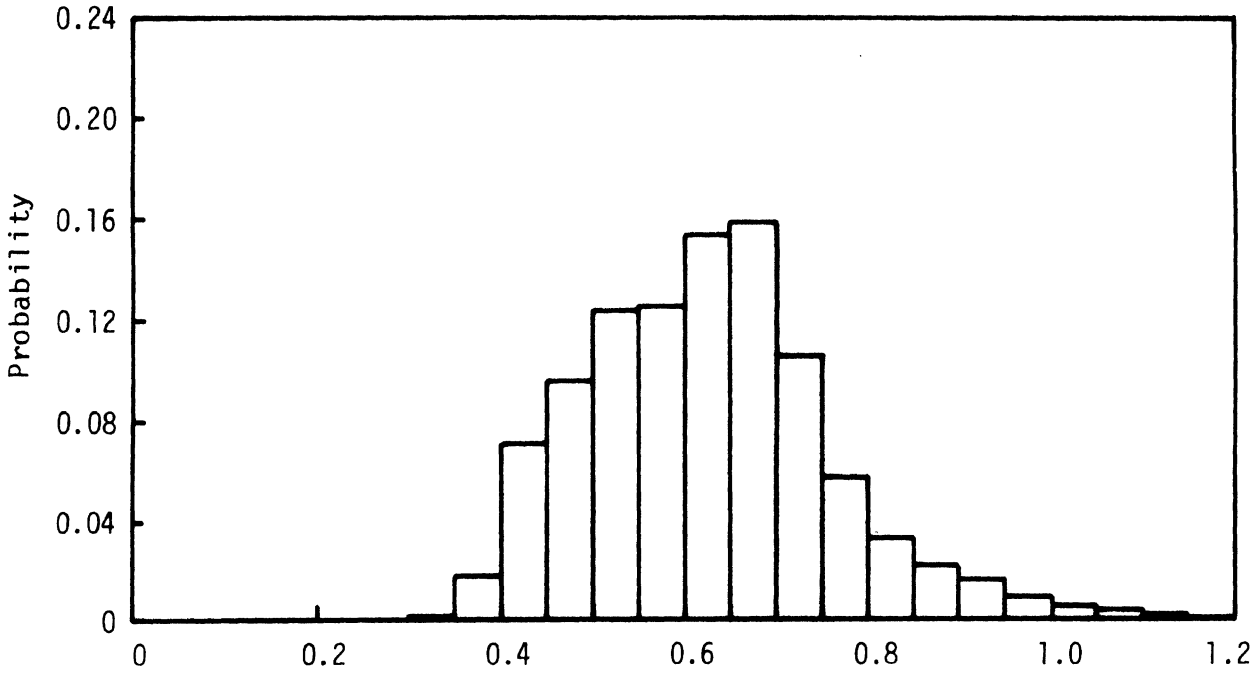

(b) Steering Sensitivity

Figure 5. Distributions of understeer and steering sensitivity for the at-risk vehicle population.

distribution is found between 0.4 and 0.8 g's/100 deg. These in-use distributions, like the OE distributions, are based on base vehicle specifications, with each occupant (or passenger) assumed to weigh 150 pounds.

The distributions of understeer and steering sensitivity in an accident-involved population are shown in Figures 6a and b. The mean value of understeer coefficient exhibited by 218 vehicles is 3.48 deg/g with the standard deviation being 1.39 deg/g. It is observed that the mean is only 0.05 deg/g (or 1.4%) lower than the mean obtained for the at-risk population. However, the standard deviation is 0.22 deg/g (or 14%) less than that exhibited by the in-use population. Further, about 90% of the distribution lies between 1 and 5.5 deg/g, a result that is quite similar to the in-use distribution of understeer. For the distribution of steering sensitivity the mean value is 0.614 g's/100 deg (at 40 mph), and the standard deviation is 0.145 g's/100 deg (at 40 mph). These values represent departures from the mean and standard deviation of the distribution for the at-risk population of 2.7% less and 5.1% greater, respectively. In addition, approximately 90% of the distribution is located between 0.4 and 0.85 g's/100 deg (at 40 mph), very much like the in-use distribution of steering sensitivity.

Despite the similarity of both the understeer and steering sensitivity distributions yielded by the accident and at-risk populations, chi-square tests for the goodness of fit of the two distributions yielded by the accident population to the distributions estimated for the at-risk populations indicated a difference in both the distributions of understeer and steering sensitivity at a level of significance of 0.05. However, with the relatively large sample sizes involved, even very slight differences can be statistically significant. From an engineering standpoint, the distributions are very similar, and any differences among the distributions are most probably inconsequential.

Consideration must also be given to the following points in comparing the distributions for the accident-involved population to those of the at-risk population. There were originally 513 vehicles in the accident sample.

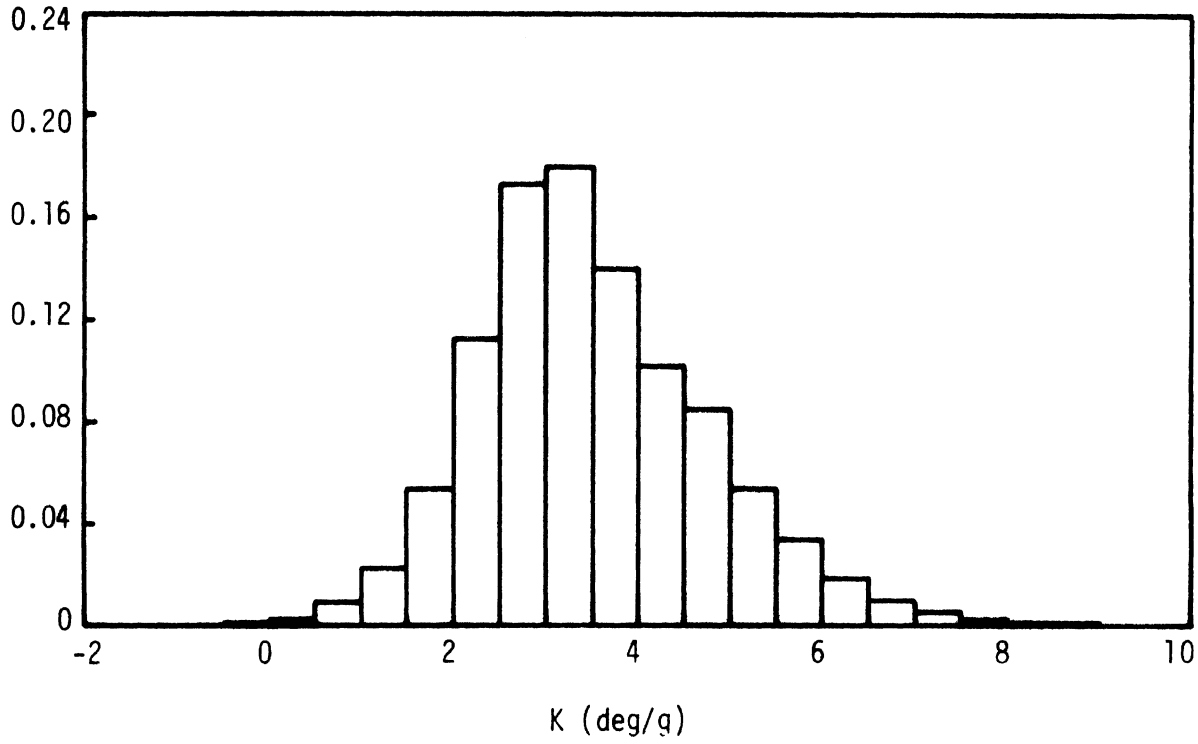

Figure 5a. (Repeated) Distribution of understeer for the at-risk population.

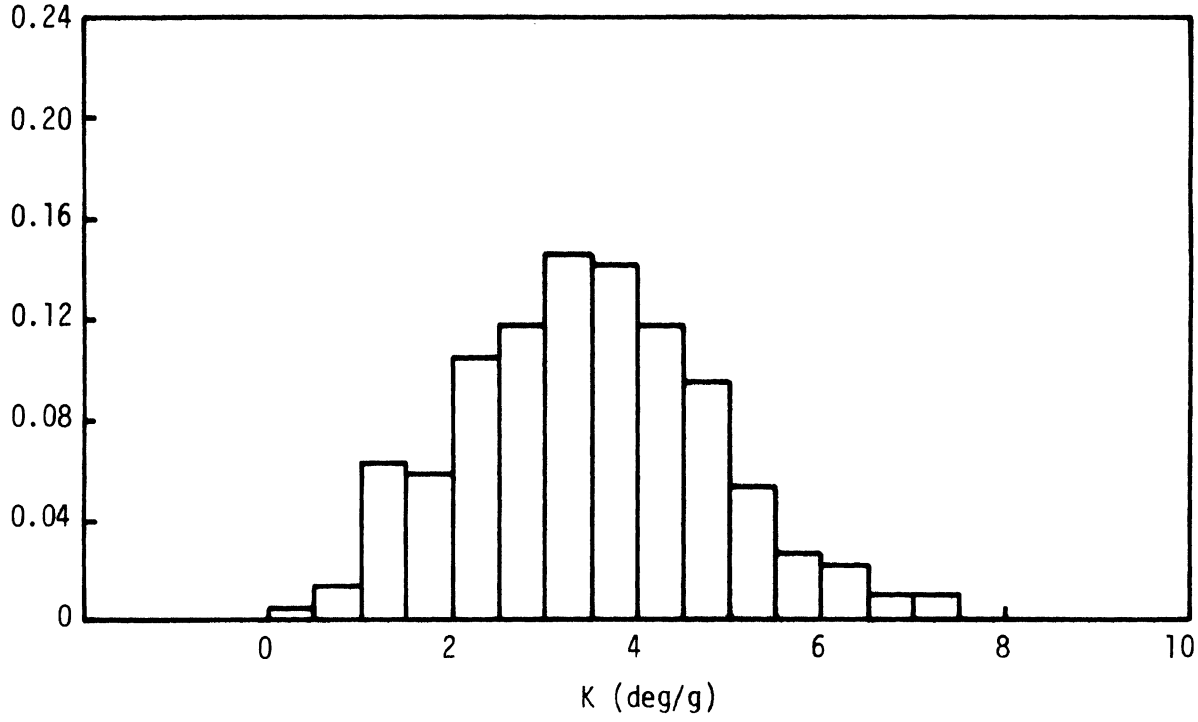

Figure 6a. Distribution of understeer for the accident-involved vehicle population.

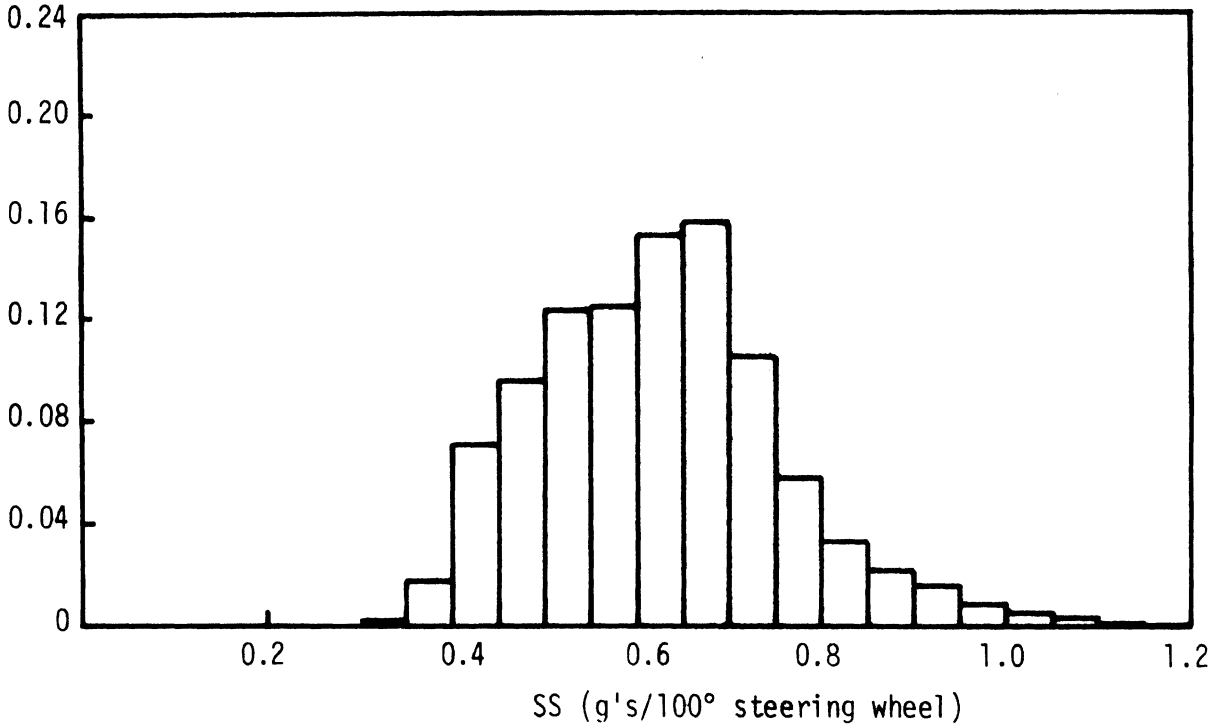

Figure 5b. (Repeated) Distribution of steering sensitivity for the at-risk population.

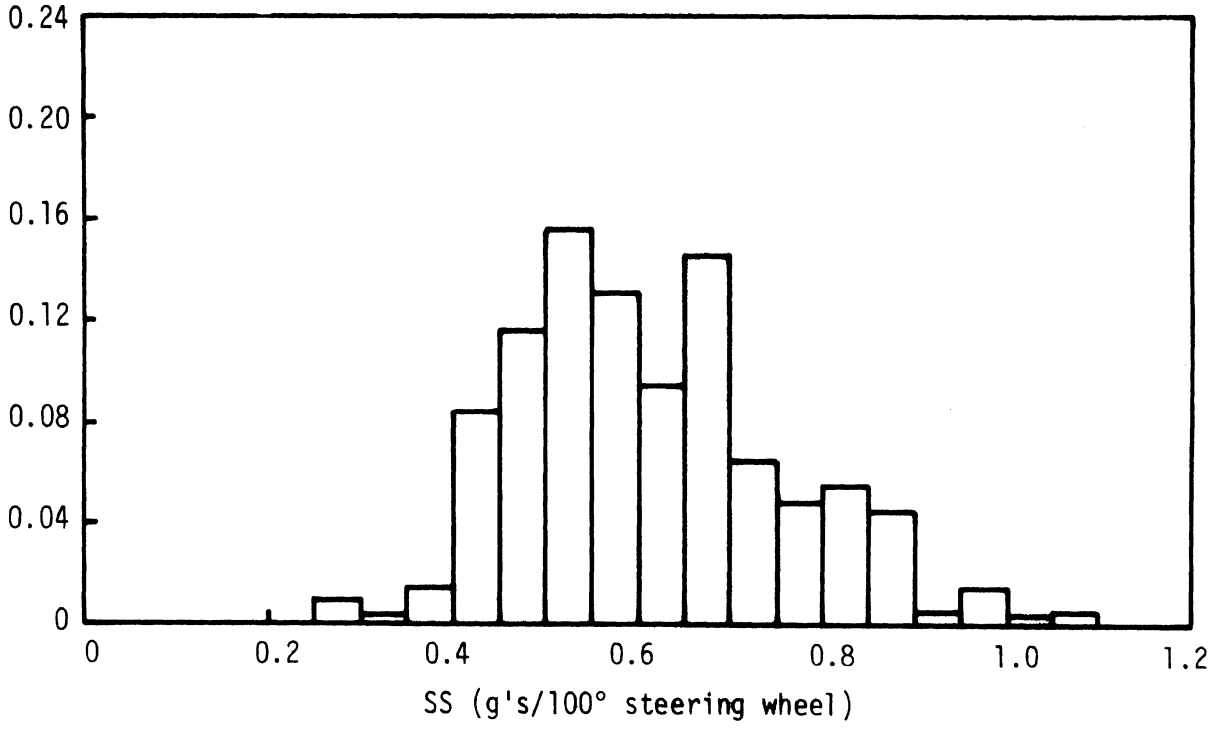

Figure 6b. Distribution of steering sensitivity for the accident-involved vehicle population.

However, eliminating foreign cars, light trucks, and cases with tires that had lost air during the accident left only 218 vehicles. A sample size of 218 seems rather small, and it is conceivable that these results could change markedly with a much larger, and therefore more representative, accident population.

It should be noted that data were available defining the actual tires (sizes, etc.) for the accident-involved vehicles. Thus, it was assumed that a more accurate estimate of understeer should try to reflect true wheel loads rather than the loads produced by assuming weights associated with the base vehicle. Accordingly, sales-weighted, average vehicle weights were computed using (1) the weights of the optional equipment tabulated in the MVMA specifications and (2) the installation rates of these various options, as can be obtained from annual production summaries. On the other hand, base vehicle weight was used to compute roll compliance, since only the spring rates associated with the base vehicle were known.

Perhaps the biggest obstacle to making a fair comparison between the at-risk and the accident populations is the manner in which tire sizes and constructions were handled. For the at-risk population, the tire size and construction associated with the base vehicle was assumed. Thus, mixing of sizes and constructions was not included in the calculations of the in-use distributions of understeer and steering sensitivity because accounting for these variables would have been rather difficult. On the other hand, the size and construction of each tire was known for each accident vehicle, and this information was used in calculating understeer for these vehicles. An examination of the data shows that the majority of vehicles had identical tire sizes and constructions at all four wheels. However, a significant number of vehicles had different tire sizes on front and rear axles (generally, bigger tires on the rear) and some had different sizes distributed more or less randomly. Mixing of radials with non-radials occurred on only one vehicle. However, mixing of bias and bias-belted tires was common, but would appear to have little

consequence as these two constructions have nearly identical stiffnesses for a given tire size.

The presence of mixed tire sizes on the accident vehicles and the assumption of the OE base vehicle tire size for the in-use calculations could, then, account for some of the difference in the respective distributions of understeer and steering sensitivity. On the whole, though, it is observed that the differences in the distributions calculated for the two populations are slight.

5.0 CONCLUSIONS AND RECOMMENDATIONS

The following conclusions can be drawn from this study:

1) The feasibility of estimating understeer coefficients using available data on tire stiffnesses and chassis parameters has been demonstrated.

2) Understeer distributions calculated for the at-risk and accident vehicle populations showed no differences of any consequence between the two.

3) Distributions of steering sensitivity calculated for the at-risk and accident vehicle populations showed no differences of any consequence between the two.

It is recommended that this study be extended and refined with particular attention being given to the following points.

1) There is a shortage of data illustrating the effects of inflation pressure and tread depth on tire stiffness properties. Testing should be carried out to better define these dependencies.

2) It is very difficult to expand the OE understeer and steering sensitivity distributions to account for the in-use mixing of tire sizes and constructions. Since these variables are important, however, it appears advisable to calculate the in-use distributions in a manner analogous to the method used for the accident distributions, namely, calculate the understeer coefficient and steering sensitivity for each vehicle in the checklane sample. The necessary tire data are known for this sample. Precautions, however, would have to be taken to assure a representative make/model distribution.

3) A much larger sample of accident vehicles would be desirable.

APPENDIX A
TIRE STIFFNESS CALCULATIONS

The tire stiffness data base employed in this study has been generated by the Calspan Corporation with the aid of their Tire Research Facility (TIRF). Mechanical characteristics were measured on 298 different passenger-car tires at a variety of normal loadings, with each tire tested at 24 psi cold inflation pressure and at full tread depth. The tests were conducted at 30 mph on a surface having a roughness equivalent to a skid number of 75.

Descriptors for each tire tested were placed in a computer file named DATA1. A sample entry for a tire showing the various descriptors is shown in Figure A.1.

Stiffness data for each tire in DATA1 was put into another computer file called DATA2. This file contained cornering and aligning moment stiffnesses for six vertical loads and inclination (camber) stiffness for five loads. The loads ranged from 50% to 175% of the rated load at 24 psi as prescribed by the Tire and Rim Association. A sample entry for a tire is shown in Figure A.2.

The procedures used to correct stiffnesses for inflation pressure and tread depth are described below.

A.1 Inflation-Pressure Correction

The correction for the effect of inflation pressure on cornering stiffness was developed from data found in the open literature for twelve tires, all of size E and H, or equivalent. (These tires are listed in Table A.1.) Two dimensionless quantities were selected to represent the data. The first was non-dimensional cornering stiffness, C_α/C_{α_o} where C_α denotes cornering stiffness and C_{α_o} denotes cornering stiffness at 24 psi and rated load. The second quantity was $\frac{p}{F_z/wd}$ where p denotes inflation pressure, F_z denotes normal load, w denotes section width, and d denotes overall diameter as listed in the T.& R.A. yearbook. This second quantity was selected to normalize

Sample Tire Descriptor List from File DATA 1

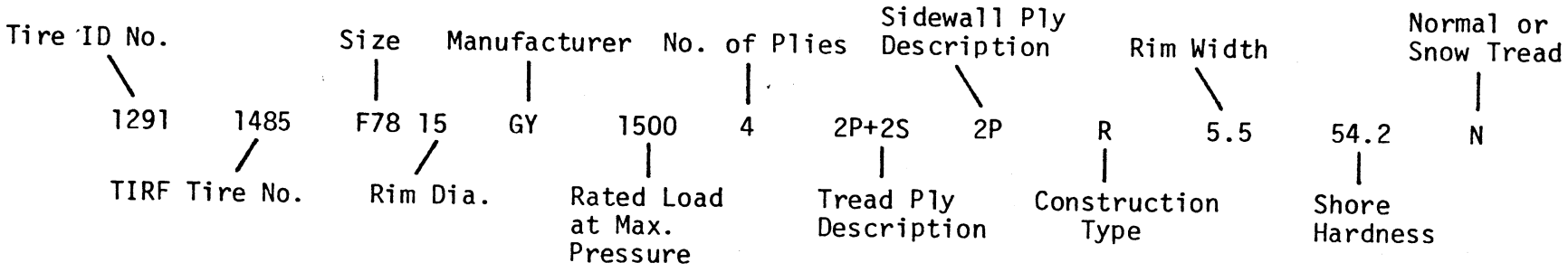

Figure A.1

Load (lb)	Cornering Stiffness (lb/deg)	Aligning Moment Stiffness (ft-lb/deg)	Camber Stiffness (lb/deg)
2750.8	168.4	74.4	50.0
2363.2	168.7	64.5	45.1
1968.3	170.3	54.6	41.9
1575.0	178.9	42.2	39.8
1184.3	179.0	30.4	35.7
791.2	153.8	17.7	0.0

Figure A.2. Sample entry for a tire from file DATA2.

Table A.1. Tires Used for Developing the Inflation Pressure Correction.

Tire	Size	Reference
BFG Silvertown	E78-14	15
Firestone 500	E78-14	15
Goodyear Custom Power Cushion Polyglas	E78-14	15
Pirelli	185R-14	15
General Belted Jumbo 780	H78-14	15
Firestone 500	H78-14	15
Firestone Town & Country Sup-R-Belt	H78-14	15
Firestone Town & Country	HR78-14	15
Firestone Deluxe Champion Sup-R-Belt	H78-14	15
Bridgestone	225R-14	15
Firestone	H78-14	
General Belted Jumbo 780	E78-14	

the data with respect to tire size. In the attempt to correlate C_α/C_{α_o} with $\frac{p}{F_z/wd}$, it was found that the quantity $(C_\alpha/C_{\alpha_o})(24/p)^{0.57}$ provides a satisfactory correlation. The relationship between these two non-dimensional numerics was found by fitting a cubic polynomial to the available data, yielding:

$$\left(\frac{C_\alpha}{C_{\alpha_o}}\right)\left(\frac{24}{p}\right)^{0.57} = 0.473 + 0.245\left(\frac{p}{F_z/wd}\right) - 0.0317\left(\frac{p}{F_z/wd}\right)^2 + 0.00109\left(\frac{p}{F_z/wd}\right)^3 \qquad (A.1)$$

The goodness of this fit is shown graphically in Figure A.3. It has a coefficient of determination, r^2, of 0.61. Further, the range of the quantity $\frac{p}{F_z/wd}$ for which this estimation is valid is 1.7 to 11.95. The range of inflation pressures in the original test data was 12 to 36 psi.

No corrections for the effect of inflation pressure on aligning stiffness or inclination stiffness were developed. Because the equation for the understeer coefficient is much less sensitive to changes in aligning moment and camber stiffnesses than it is to changes in cornering stiffnesses, the lack of corrections for these parameters is not viewed as a serious shortcoming.

A.2 Tread Depth Correction

Data showing the influence of tread depth on tire stiffnesses was even more sparse than inflation pressure data. Data was located only for the five tires listed in Table A.2. Generally speaking, both cornering and aligning-moment stiffness increase with decreasing tread depth, but the magnitude of the increase is dependent on vertical load. This behavior is illustrated in Figures A.4a-d.

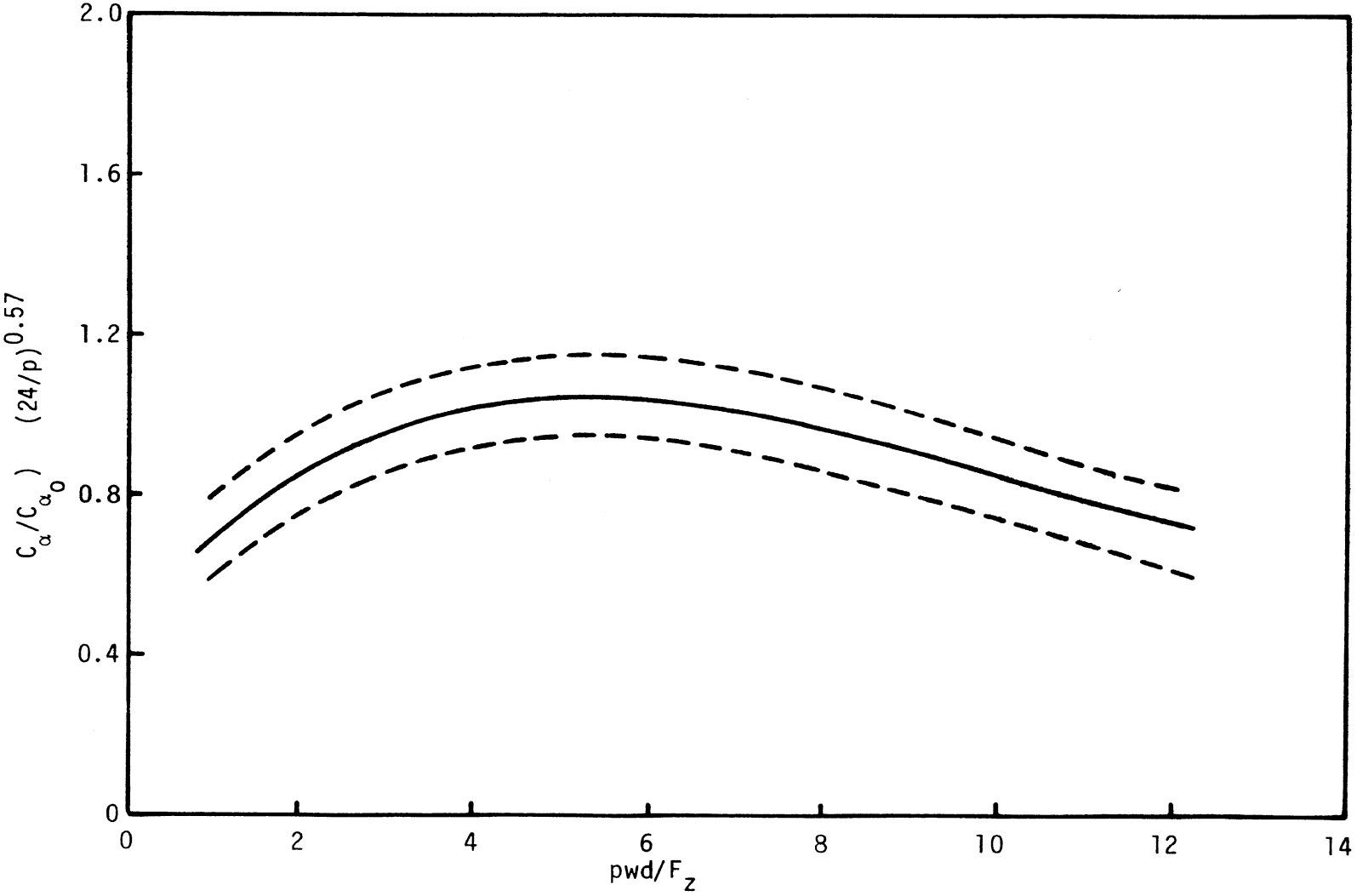

Figure A.3. Inflation pressure correction for cornering stiffness.

Table A.2. Tires Used for Developing the Tread Depth Corrections.

Tire	Size	Reference
Firestone Deluxe Champion Sup-R-Belt	G78-14	5
Firestone Radial Deluxe Champion	GR78-14	5
Firestone 500	E78-14	15
Firestone Sup-R-Belt	H78-14	15
	8.55-14	

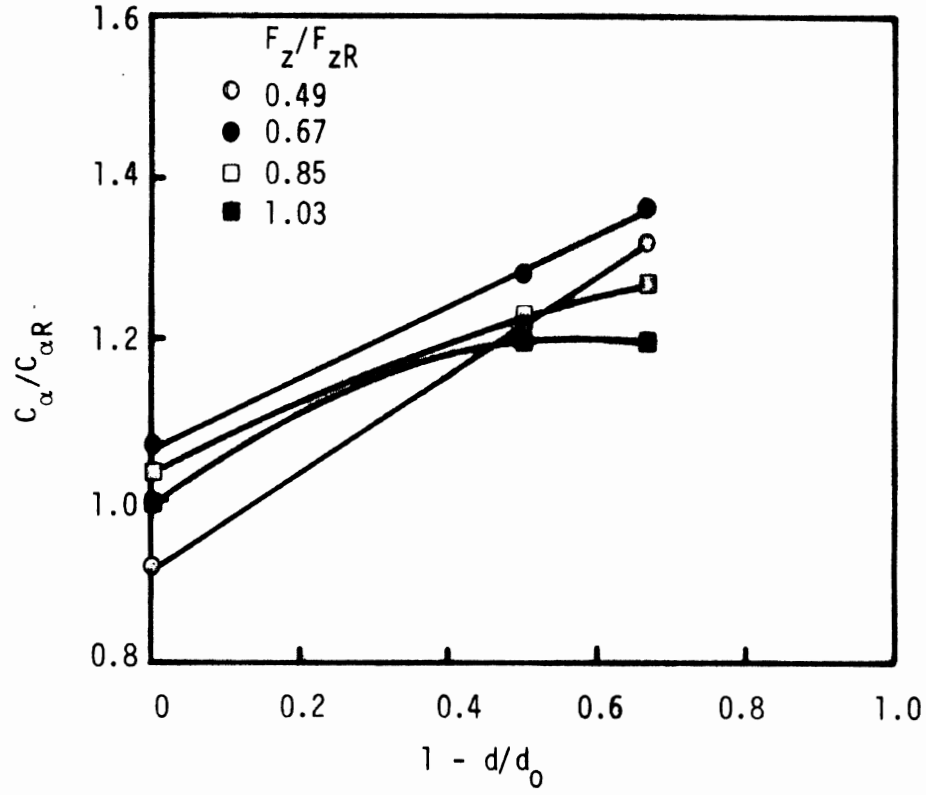

(a) Cornering Stiffness vs. Tread Wear

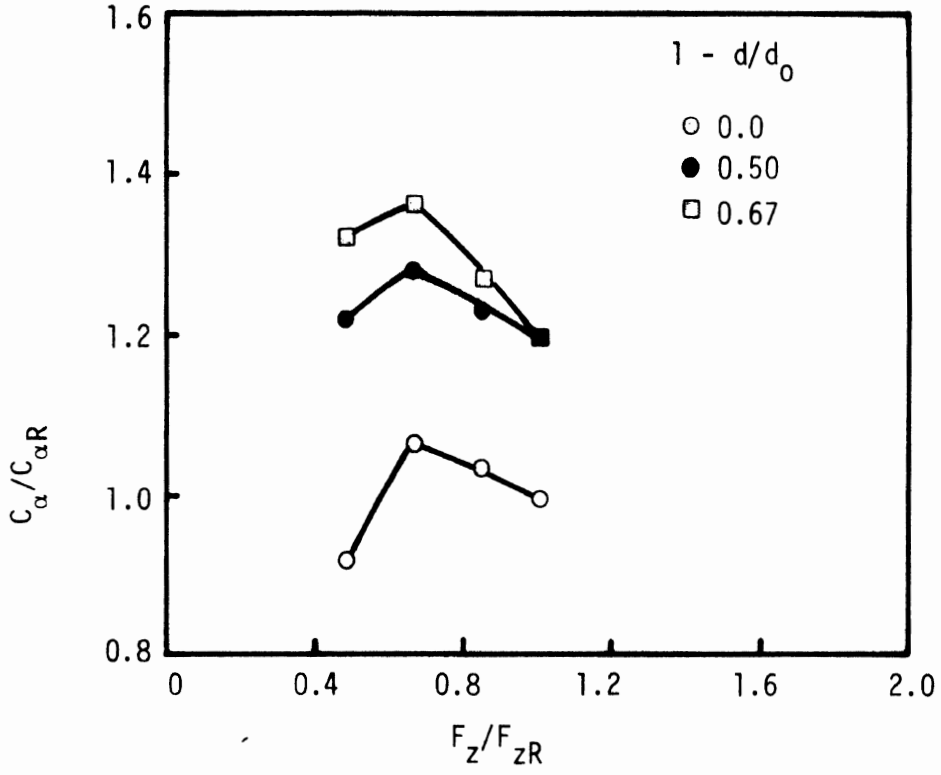

(b) Cornering Stiffness vs. Load

Figure A.4. Cornering and aligning moment stiffness as a function of tread depth and load for a typical tire.

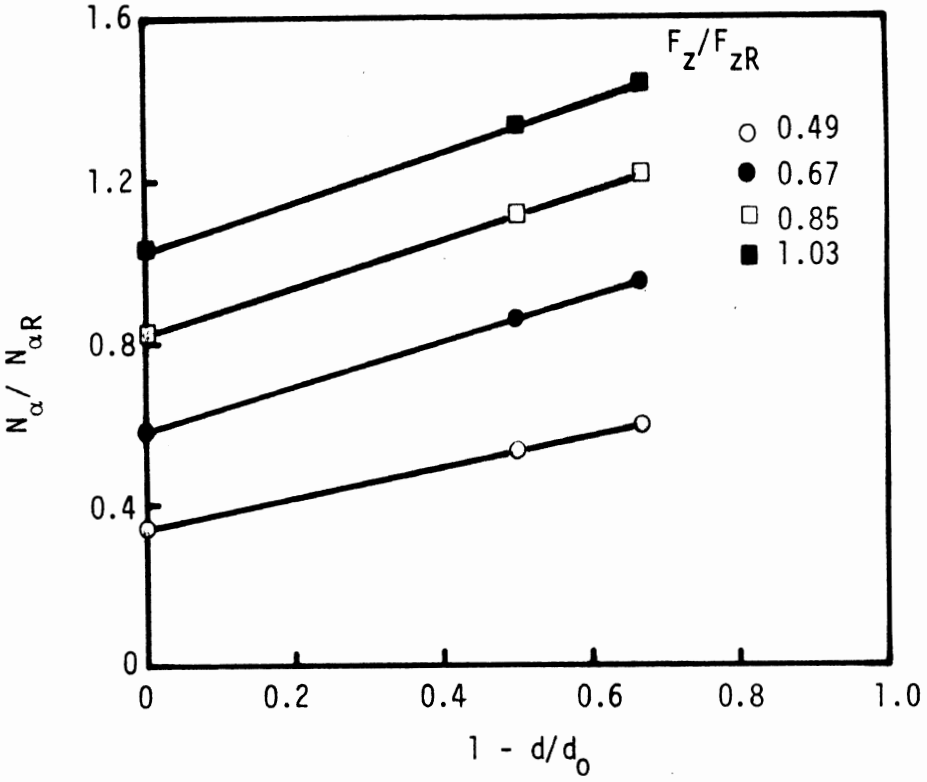

(c) Aligning Moment Stiffness vs. Tread Wear

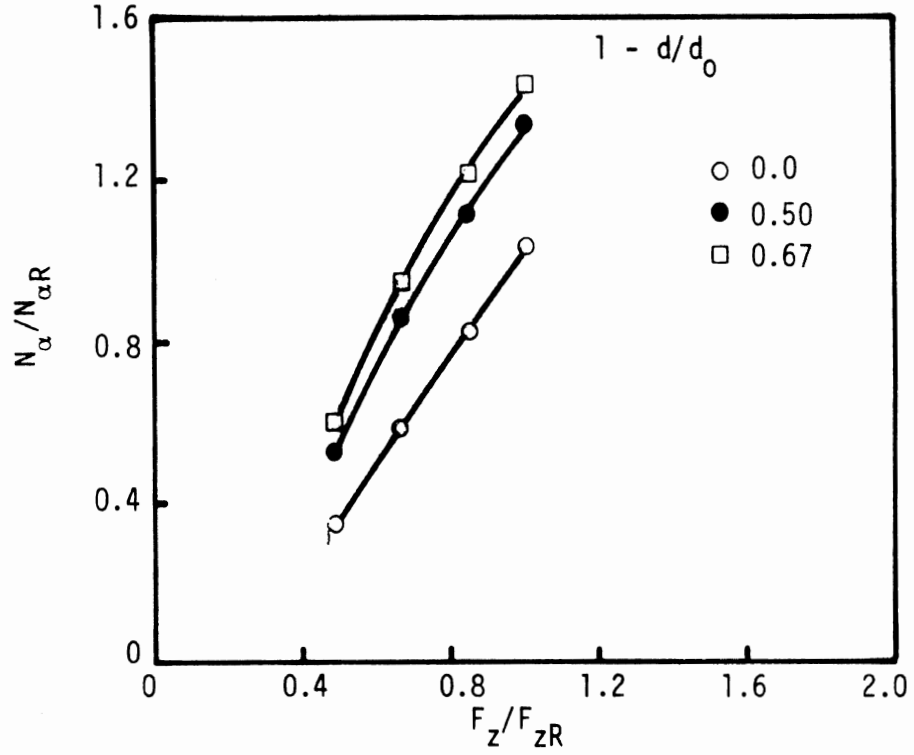

(d) Aligning Moment Stiffness vs. Load

Figure A.4 (Cont.)

To derive a correction for cornering stiffness, the data were grouped in terms of three dimensionless parameters: (1) a dimensionless cornering stiffness, C_α/C_{α_R}, where C_α denotes cornering stiffness and C_{α_R} denotes cornering stiffness at the tire's cold inflation pressure and corresponding rated load; (2) the fraction of tread worn away, $1 - d/d_o$, where d denotes tread depth and d_o denotes full tread depth; and (3) a dimensionless load, F_z/F_{z_R}, where F_z denotes load and F_{z_R} denotes rated load at the tire's cold inflation pressure. Dimensionless cornering stiffness appeared to be related in a parabolic manner to both fractional tread depth and dimensionless load. Accordingly, a least squares curve fit was performed yielding the following relationship:

$$\frac{C_\alpha}{C_{\alpha_R}} = 0.530 + 0.957\left(\frac{F_z}{F_{z_R}}\right) - 0.472\left(\frac{F_z}{F_{z_R}}\right)^2 + 0.939\left(1 - \frac{d}{d_o}\right) - 0.340\left(1 - \frac{d}{d_o}\right)\left(\frac{F_z}{F_{z_R}}\right) - 0.259\left(1 - \frac{d}{d_o}\right)^2 \qquad (A.2)$$

The coefficient of determination, r^2, of this fit is 0.83, with the equation being valid for tread depths ranging from full to bald and dimensionless loads ranging between 0.25 and 1.75.

The radial tire was not included in this curve fit because it exhibited marked differences from the other tires. It was found that the cornering stiffness of this one tire was not particularly affected by tread depth, especially at high loads. To base a correction for radial tires on this one tire appeared rather questionable, so, instead, the correction equation (A.2) was applied to all tires regardless of construction type.

A procedure for correcting aligning stiffness for tread depth was also developed. A dimensionless aligning moment stiffness, N_α/N_{α_R},

analogous to dimensionless cornering stiffness, and the numerics defining fraction of tread worn away and dimensionless load are employed, as before. A satisfactory curve fit to the data was obtained by assuming dimensionless aligning stiffness to vary in a linear fashion with fractional tread depth and parabolically with dimensionless load. The resulting equation is

$$\frac{N_\alpha}{N_{\alpha_R}} = -0.467 + 1.794\,\frac{F_z}{F_{z_R}} - 0.301\left(\frac{F_z}{F_{z_R}}\right)^2 + 0.250\left(1 - \frac{d}{d_o}\right) + 0.725\left(1 - \frac{d}{d_o}\right)\frac{F_z}{F_{z_R}} - 0.372\left(1 - \frac{d}{d_o}\right)\left(\frac{F_z}{F_{z_R}}\right)^2 \qquad (A.3)$$

The coefficient of determination, r^2, is 0.97. The equation is valid for tread depths ranging from full to bald and dimensionless loads ranging from 0.4 to 1.75.

In contrast to the manner in which the cornering stiffness of the radial tire varied with tread depth, the aligning stiffness of the radial tire varied with tread depth in a manner similar to the other tires, and consequently, Equation (A.3) applies to all tires. However, aligning moment data were not available for the 8.55-14 bias-ply tire, and thus this tire did not enter into the derivation of Equation (A.3).

A correction for the effect of tread depth on inclination (camber) stiffness was not developed. Its omission is justified on the grounds that the understeer coefficient is not nearly as sensitive to changes in inclination stiffness as it is to changes in cornering stiffness.

A.3 Applying the Stiffness Corrections

Because of the way the tire stiffnesses were normalized in the correction equations, the following procedure was used to implement the corrections.

For a given tire, the cornering stiffness at 24 psi and at rated load is obtained from the Calspan test data by averaging the stiffness of all tires of the same size and construction. The inflation pressure correction is then applied to obtain cornering stiffness at the actual inflation pressure of the tire and the rated load at that pressure. There were a few cases in the in-use inflation pressure distribution where the pressure was outside the range of the table of T. & R.A. rated loads. In these cases, extrapolations were made for rated load. The tread depth correction was then applied using the fractional tread depth and actual load carried by the tire. (Thus, the influence of load on cornering stiffness is handled by the tread depth correction.) For purposes of the calculation, a full tread depth of 12/32" was assumed.

The procedure for aligning moment stiffness was analogous to that for cornering stiffness except that no pressure correction was made. Therefore, an inflation pressure of 24 psi was assumed.

Inclination stiffness was not adjusted for inflation pressure or tread depth. Instead, this parameter was obtained for the appropriate load directly from the Calspan test data.

It should be noted that the corrections were applied to all tires even if they had an inflation pressure of 24 psi and full tread depth and could have been obtained directly from the Calspan data. This was done so that every tire would be treated consistently, and no confusion would result from using two or more methods to calculate stiffnesses.

APPENDIX B

ROLL CAMBER RATE, FRONT ALIGNING MOMENT COMPLIANCE STEER, AND ROLL COMPLIANCE

This appendix documents the manner in which chassis parameters were obtained for use in the understeer equation.

B.1 Roll Camber Rate of the Front Suspension

Values of front-wheel roll camber rate, $\partial\gamma/\partial\phi$, were found in the open literature for eight vehicles. The median value (0.90 deg/deg) of the data tabulated in Table B.1 was adopted (as discussed earlier) as a value representative of all vehicles.

B.2 "Front Wheel Aligning Moment Compliance Steer"

Values of "front aligning moment compliance steer," as needed for Equation (1), cannot be found, as such, in the literature. However, data could be found for nine vehicles in terms of steering system stiffness, which parameter is simply the reciprocal of the total aligning moment compliance steer, $\partial\psi/\partial M_{zF}$, of the front axle, i.e., twice the "aligning moment compliance steer" for a single front wheel. Examination of the measured values of compliance steer listed in Table B.2 shows the median value to be 0.54 deg/100 ft-lb, which value was assumed, in this study, to be representative of motor cars, in general.

B.3 Roll Compliance

Roll compliance was estimated from data provided in the MVMA specification sheets. Given that roll compliance may be expressed as

Table B.1. Various Measured Values of Front Suspension Roll Camber Rate.

Vehicle	Roll Camber Rate $\frac{\partial \gamma}{\partial \phi}$ (deg/deg)	Reference
1971 Buick Century	1.00	15
1971 Chevrolet Brookwood	0.76	16, 17
1971 Dodge Coronet	0.91	16, 17
1971 Ford Mustang	0.76	16
1971 Oldsmobile F-85	0.76	16
1971 Pontiac Firebird	0.94	17
1969 Ford Galaxie	0.89	8
1970 Ford Torino	1.01	9

median = 0.90 deg/deg

Table B.2. Various Measures of Front Aligning Moment Compliance Steer.

Vehicle	Front Aligning Moment Compliance Steer $\frac{\partial \psi}{\partial M_{zF}}$ (deg/100 ft-lb)	Reference
1971 Ford Mustang	0.38	15, 16
1973 Buick Century	0.92	15
1971 AMC Ambassador	0.54	16
1971 Dodge Coronet	0.65	16, 17
1971 Oldsmobile F-85	0.38	16
1971 Chevrolet Brookwood	0.40	17
1971 Pontiac Firebird	0.43	17
1969 Ford Galaxie	1.21	8
1970 Ford Torino	0.88	9

median = 0.54 deg/100 ft-lb

$$\frac{\partial \phi}{\partial a_y} = \left[\frac{W_s h}{\left(\left. \frac{\partial L}{\partial \phi} \right|_F + \left. \frac{\partial L}{\partial \phi} \right|_R \right) \left(\frac{180}{\pi} \right) - W_s h} \right] \left(\frac{180}{\pi} \right) \text{ deg/g} \qquad \text{(B.1)}$$

where

$\frac{\partial \phi}{\partial a_y}$ = roll compliance (deg/g)

W_s = sprung weight (lb)

h = distance from sprung mass c.g. to roll axis (ft)

$\left. \frac{\partial L}{\partial \phi} \right|_{F,R}$ = front and rear suspension roll stiffness, respectively (ft-lb/deg)

it is necessary to compute, or estimate, the quantities on the right-hand side of Equation (B.1).

Since

$$W_s = W_{Vs} + W_L \quad \text{lb} \qquad \text{(B.2)}$$

where W_{Vs} = sprung weight of vehicle (lb)

and W_L = weight of occupants (lb)

a method is needed to obtain W_{Vs} for each vehicle. A least squares fit of the data shown in Table B.3 yielded the following relationship:

$$W_{Vs} = 0.884 W_T - 127 \quad \text{lb} \qquad \text{(B.3)}$$

where W_T = base vehicle curb weight (lb).

The distance, h, was estimated with the following relationship:

$$h = 0.31\, h_{ov} \quad \text{ft} \qquad \text{(B.4)}$$

Table B.3. Base Vehicle Curb Weights and Sprung Weights.

Vehicle	Base Vehicle Weight (lb)	Sprung Weight (lb)	Reference
	2690	2231	18
	2790	2332	18
	2910	2436	18
	3100	2636	18
	3220	2745	18
	3590	3068	18
	3770	3218	18
	4150	3516	18
	4180	3604	18
	4370	3804	18
	4470	3816	18
1969 Chevrolet	3660	3094	18
1969 Chevrolet Malibu	3140	2656	18
1969 Chevrolet Nova	2910	2425	18
1969 Chevrolet Camaro	3120	2617	18
1969 Pontiac Grand Prix	3885	3356	18
1969 Pontiac Firebird	3218	2695	18
1969 Buick Special	3248	2735	18
1969 Buick	4088	3456	18
1969 Oldsmobile	4001	3422	18
1969 Oldsmobile Cutlass	3231	2749	18
1969 Cadillac	4756	4082	18
1969 Ford Galaxie	3782	3220	18
1973 Plymouth Valiant	2965	2490	18
1973 Dodge Coronet	3505	2945	18
1973 Chrysler	4280	3610	18
1974 Ford Pinto	2440	2074	18
1974 Ford Maverick	2839	2364	18
1974 Ford Torino	3881	3269	18
1974 Ford	4302	3653	18

Table B.3. (Cont.)

Vehicle	Base Vehicle Weight (lb)	Sprung Weight (lb)	Reference
1971 AMC Ambassador	3384	2832	16
1971 Chevrolet Brookwood	4646	3998	16
1971 Dodge Coronet	3385	2863	16
1971 Ford Mustang	3151	2659	16
1971 Oldsmobile F-85	3358	2819	16
1971 Pontiac Firebird	3240	2703	17
1973 Chevrolet Caprice	4856	4115	7
1974 Chevrolet Nova	3364	2810	7
1967 Ford	4257	3707	19
1970 Ford Torino	3258	2784	9
1970 Chevrolet	4333	3657	20
1972 Chevrolet	4808	4091	20
1972 Chevrolet	3983	3491	20

where h_{ov} = overall vehicle height (ft)

Equation (B.4) was derived by calculating the length, h, from data defining the center of gravity location for several vehicles, as found in the literature. The location of the roll axis was either given or assumed to be at ground level at the front axle and of wheel center height at the rear axle. Overall vehicle height is obtained from the MVMA specification sheets. The data used for the analysis is presented in Table B.4.

The roll stiffness of the front suspension was estimated by using the following relationship:

$$\left.\frac{\partial L}{\partial \phi}\right|_F = \frac{1}{2} t^2 K_F \left(\frac{\pi}{12 \cdot 180}\right) + \left.\frac{\partial L_{aux}}{\partial \phi}\right|_F \quad \text{ft-lb/deg} \qquad (B.5)$$

where

t = track (in)

K_F = spring rate at front wheel (lb/in) (base vehicle)

$\left.\frac{\partial L_{aux}}{\partial \phi}\right|_F$ = auxillary roll stiffness (ft-lb/deg) of the front suspension.

Auxillary roll stiffness derives from sources other than the vertical springing with the major contributor being the anti-roll bar or roll stabilizer. In the absence of an anti-roll bar, the auxillary roll stiffness of the front suspension was estimated to be 34 ft-lb/deg, a value that is the average of the vehicles listed in Table B.5. Since insufficient data were available to develop a relationship between the diameters of anti-roll bars and auxillary roll stiffness, the presence of an anti-roll bar was assumed to add additional roll stiffness equal to that provided by the normal springing [18]. Thus, with an anti-roll bar fitted, it was assumed that

$$\left.\frac{\partial L_{aux}}{\partial \phi}\right|_F = \frac{1}{2} t^2 K_F \left(\frac{\pi}{12 \cdot 180}\right) + 34 \quad \text{ft-lb/deg} \qquad (B.6)$$

Table B.4. Measured Ratios of Roll Moment Arm to Overall Vehicle Height.

Vehicle	Roll Moment Arm h (in)	Overall Height h_{ov} (in)	h/h_{ov}	Reference
1971 Ford Mustang	16.9	50.5	0.33	15, 16
1973 Buick Century	22.6	55.5	0.41	15
1971 AMC Ambassador	19.2	55.2	0.35	16
1971 Chevrolet Brookwood	14.9	57.1	0.26	16, 17, 21
1971 Dodge Coronet	16.3	53.1	0.31	16, 17, 21
1971 Oldsmobile F-85	13.4	53.2	0.25	16
1971 Pontiac Firebird	11.5	50.4	0.23	17, 21
1973 Chevrolet Caprice	15.3	57.9	0.26	7
1967 Ford Galaxie	15.5	55.7	0.28	19
1969 Ford Galaxie	16.5	54.1	0.31	8
1970 Ford Torino	16.5	52.3	0.32	9
1970 Chevrolet	18.1	57.1	0.32	20
1972 Chevrolet	18.1	57.1	0.32	20
1972 Chevrolet	20.0	53.6	0.37	20

median = 0.31

Table B.5. Measured Values of Front Auxillary Roll Stiffness in the Absence of an Anti-Roll Bar.

Vehicle	Roll Stiffness $\left.\frac{\partial L_{aux}}{\partial \phi}\right\|_F$ (ft-lb/deg)	Reference
1974 Ford Pinto	18	18
1963 Pontiac	23	18
1971 Dodge Coronet	60	17

Mean = 34 ft-lb/deg

Estimation of the roll stiffness contributed by the rear suspension is complicated by the fact that it is dependent on the spacing of the rear springs used on live axle suspensions. Spring spacing, in turn, is typically dependent on the type of spring employed. Accordingly, the procedure used to estimate the roll stiffness of the rear suspension employs the following definition:

$$\left.\frac{\partial L}{\partial \phi}\right|_R = \frac{1}{2} t_s^2 K_R \left(\frac{\pi}{12 \cdot 180}\right) + \left.\frac{\partial L_{aux}}{\partial \phi}\right|_R \quad \text{ft-lb/deg} \qquad (B.7)$$

where

t_s = spring spacing (in)

K_R = spring rate at the rear wheel (lb/in) (base vehicle)

$\left.\frac{\partial L_{aux}}{\partial \phi}\right|$ = auxillary roll stiffness (ft-lb/deg) of the rear suspension

Analysis of the data presented in Table B.6a-d provided the following numbers:

Table B.6a. Measured Values of Rear Track and Rear Spring Spacing for Leaf Spring Suspensions.

Vehicle	Rear Track t_r (in)	Rear Spring Spacing t_s (in)	t_s/t_r	Reference
1963 Ford Galaxie	60.5	46.5	0.77	18
1973 Plymouth Valiant	55.6	43.0	0.77	18
1973 Dodge Coronet	62.0	47.3	0.76	18
1973 Chrysler	63.4	47.3	0.75	18
1974 Ford Pinto	55.0	42.2	0.77	18
1974 Ford Maverick	56.5	42.8	0.76	18
1971 Ford Mustang	61.0	43.0	0.71	15
1971 Chevrolet Brookwood	64.0	45.1	0.71	16, 17
1971 Dodge Coronet	62.0	47.1	0.76	16, 17
1971 Pontiac Firebird	60.4	45.5	0.75	17
1973 Chevrolet Caprice	64.0	46.8	0.73	7
	Mean = 0.77			

Table B.6b. Measured Values of Rear Track and Rear Spring Spacing for Coil Spring Suspensions.

Vehicle	Rear Track t_r (in)	Rear Spring Spacing t_s (in)	t_s/t_r	Reference
1963 Pontiac	59.3	42.0	0.71	18
1974 Ford Torino	62.9	33.7	0.54	18
1974 Ford LTD	64.3	38.4	0.60	18
1971 Buick Century	60.7	41.0	0.68	15
1971 AMC Ambassador	60.0	33.8	0.56	16
1971 Oldsmobile F-85	59.0	35.5	0.60	16
1969 Ford Galaxie	64.0	38.4	0.60	8
	Mean = 0.61			

Table B.6c. Measured Values of Rear Auxillary Roll Stiffness for Leaf Spring Suspensions.

Vehicle	Rear Auxillary Roll Stiffness $\left.\frac{\partial L_{aux}}{\partial \phi}\right\|_R$ (ft-lb/deg)	Reference
1973 Plymouth Valiant	77	18
1973 Dodge Coronet	132	18
1973 Chrysler	97	18
1974 Ford Pinto	43	18
1974 Ford Maverick	67	18

Mean = 83 ft-lb/deg

Table B.6d. Measured Values of Rear Auxillary Roll Stiffness for Leaf Spring Suspensions.

Vehicle	Rear Auxillary Roll Stiffness $\left.\frac{\partial L_{aux}}{\partial \phi}\right\|_R$ (ft-lb/deg)	Reference
1974 Ford Torino	31	18
1974 Ford Galaxie	54	18
1971 Oldsmobile F-85	84	16

Mean = 56 ft-lb/deg

Leaf-Spring Suspensions:

$$t_s = 0.77t \text{ in.} \tag{B.8a}$$

where t = track (in)

and

$$\left.\frac{\partial L_{aux}}{\partial \phi}\right|_R = 83 \text{ ft-lb/deg} \tag{B.8b}$$

Coil Spring Suspensions:

$$t_s = 0.61t \text{ in.} \tag{B.8c}$$

and

$$\left.\frac{\partial L_{aux}}{\partial \phi}\right|_R = 56 \text{ ft-lb/deg} \tag{B.8d}$$

Unfortunately, it was not possible to verify the accuracy of the above-defined roll compliance estimation procedure in view of the lack of data in the open literature. However, the values computed for the OE vehicle population ranged from about 4 to 12 deg/g with a mean of approximately 8 deg/g. These predictions appear to be very reasonable.

For many vehicles (approximately 20 percent of the OE population) spring rates were not listed, and, in these cases, the average roll compliance of 8 deg/g was assumed to exist.

APPENDIX C

VEHICLE PARAMETER ASSEMBLY

This appendix describes the compilation of vehicle specifications taken from the MVMA specification sheets, and the set of parameters applicable to the accident-involved vehicle population.

C.1 MVMA Vehicle Specifications

Many of the parameters needed by the understeer calculation were taken from the MVMA specification sheets and written onto the special coding form illustrated in Figure C.1. This form also included the installation rates for certain optional equipment elements. The information compiled on the code sheets was then keypunched and read into a computer file named CARPARAM. (It should be noted that a few parameters, not recorded on the code sheets, had to be added to the file after it was created.) A sample entry from CARPARAM is shown in Figure C.2.

C.2 Accident Vehicle Parameters

Tire sizes, inflation pressures and tread depths, and the weights of occupants in each accident case investigated by the Systems Analysis Division of HSRI were put into a file named ACC.CASES, in which each vehicle was identified only by its Vehicle Identification Number (VIN). The VIN's were decoded by a computer program called VINDICATOR '77 [22] to obtain the necessary make/model/year information. A total of 218 vehicles are contained in this file. A sample entry for a given vehicle is shown in Figure C.3.

MVMA #4.29 Vehicle Data Sheet

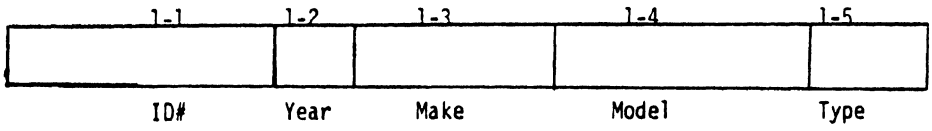

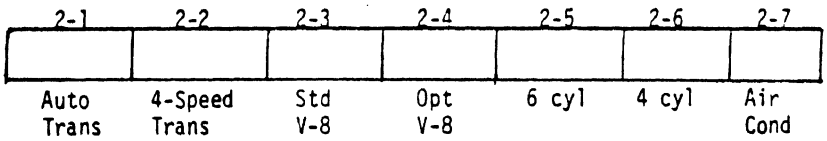

OPTION PERCENTAGES

Table 3-1; Option Weights

Option	Front	Rear	Total
Auto. Trans.			
4-Speed Trans.			
Small V-8			
Large V-8			
6-Cylinder			
Air Conditioning			

Table 3-2; Corrected Option Weights

Option	Front	Rear	Total
Auto. Trans.			
4-Speed Trans.			
Ave. Opt. V-8			
6-Cylinder			
Air Conditioning			
	3-1	3-2	3-3

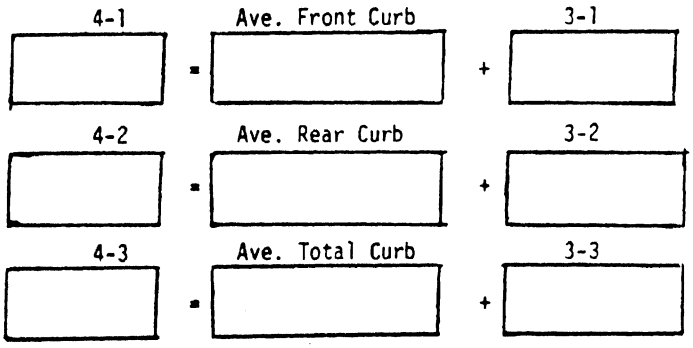

Figure C.1. Vehicle specification coding form.

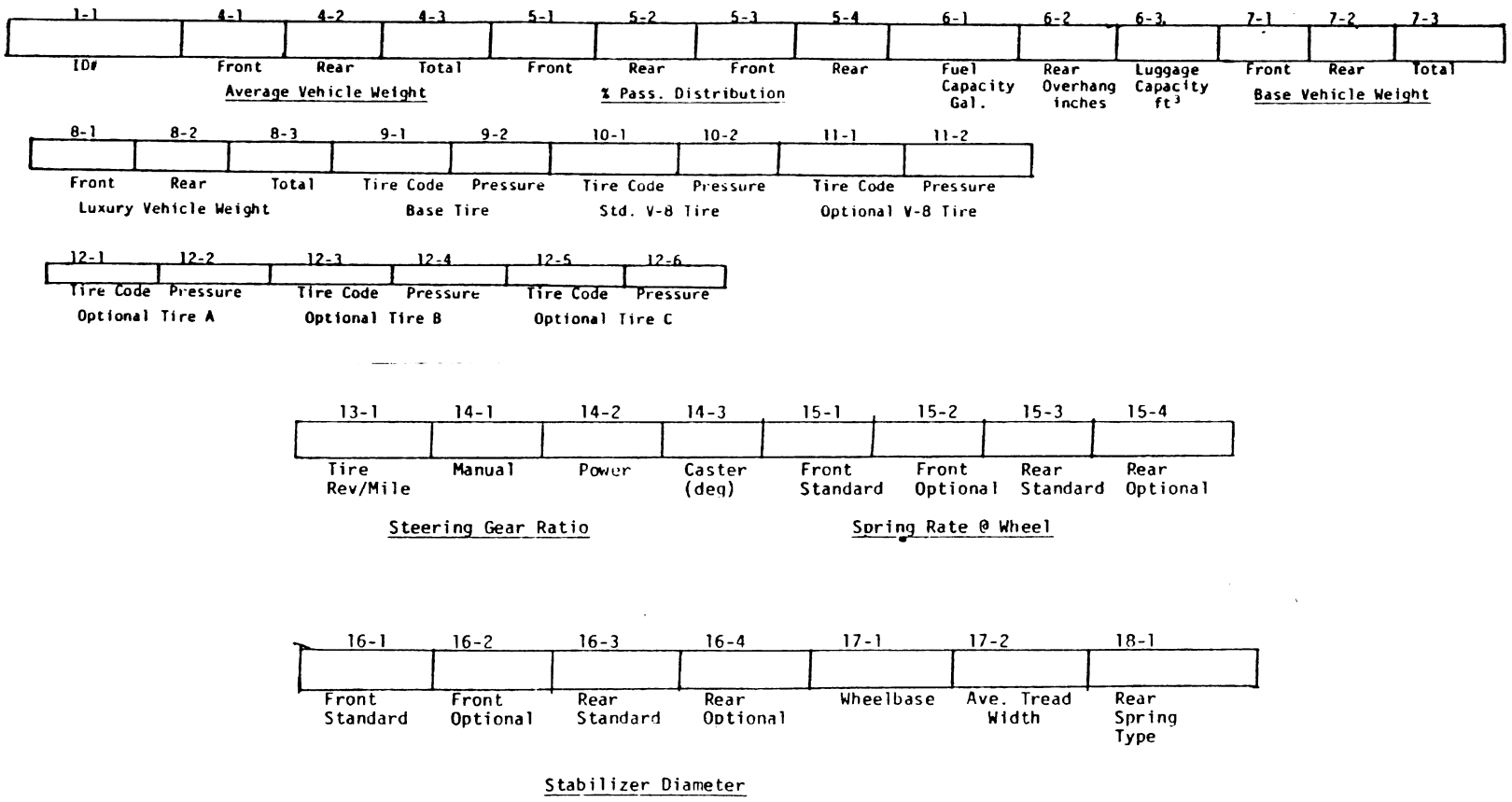

Figure C.1 (Cont.)

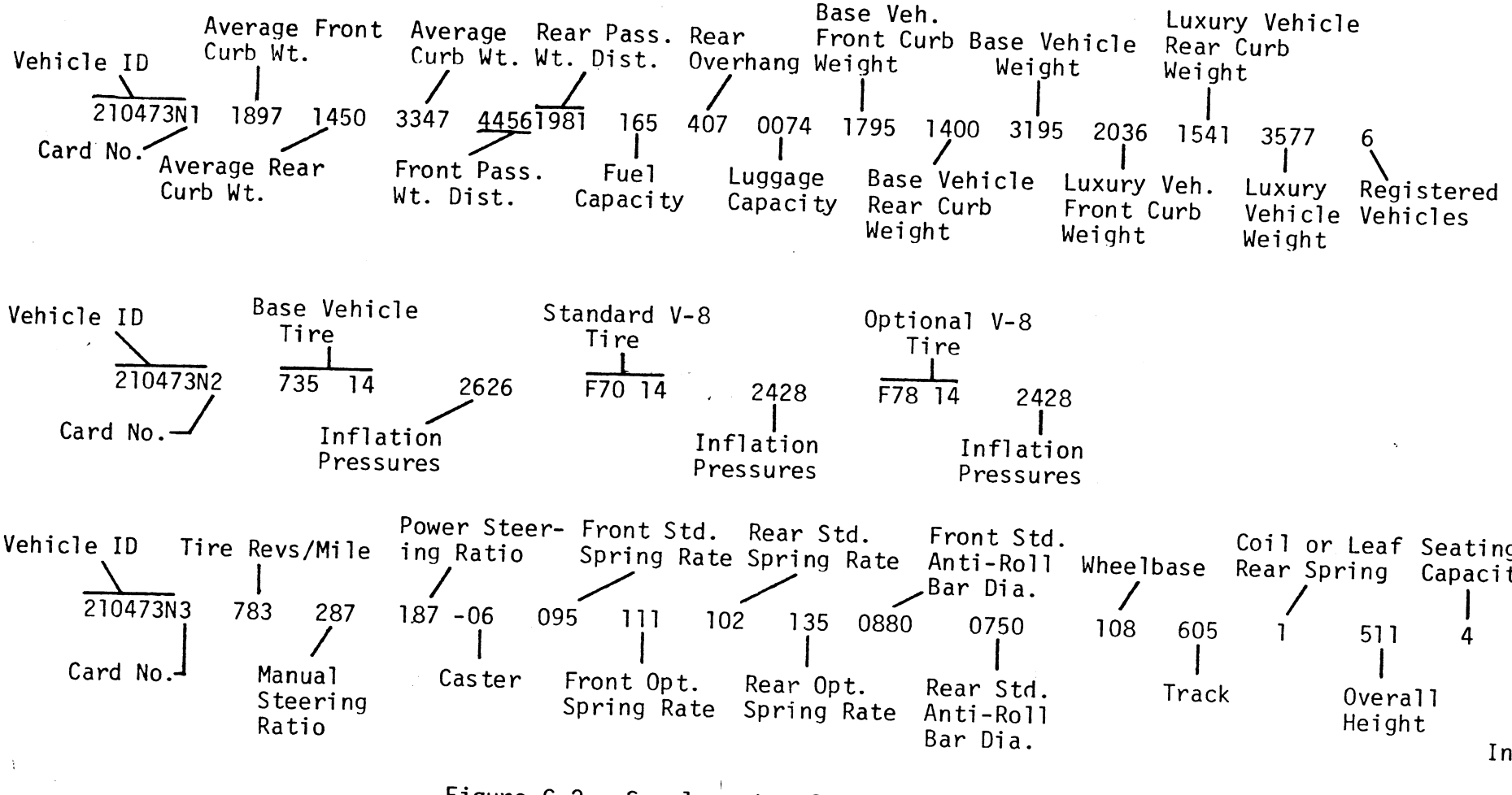

Figure C.2. Sample entry from file CARPARAM.

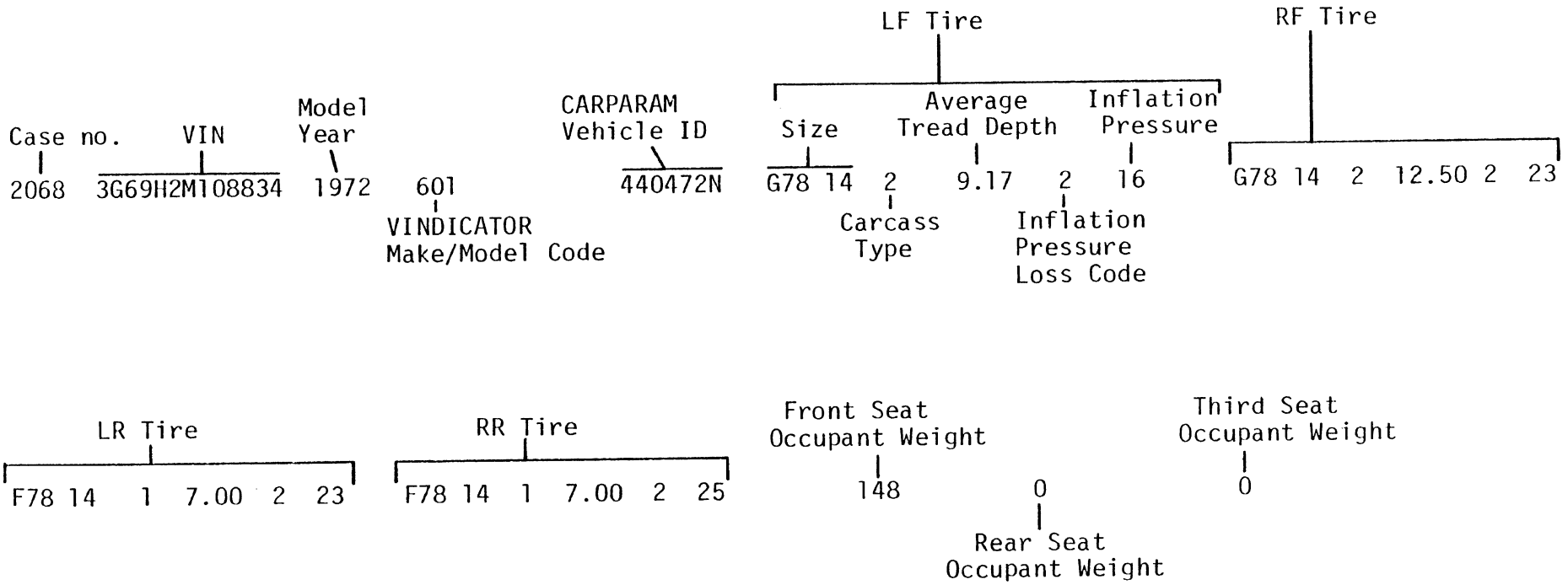

Figure C.3. Sample entry from file ACC.CASES

APPENDIX D

METHODOLOGY TO DEFINE DISTRIBUTIONS OF IN-USE INFLATION PRESSURE, TREAD DEPTH, AND LOADING

D.1 Distribution of Inflation Pressure and Tread Depth

An investigation of the inflation pressure and tread depth data from the checklane sample was conducted to determine whether vehicle age, size, or type (i.e., station wagon or non-station wagon) had any influence on the pressure-tread depth distribution. The variables investigated were average inflation pressure, front-to-rear pressure differential (average front minus average rear), average tread depth, and front-to-rear tread depth differential (average front minus average rear). All the statistical analyses were performed using the Kruskal-Wallis test, a non-parametric, rank sum test for comparing two or more samples [23]. The level of significance used for each test was 0.05.

Sample sizes, means, and standard deviations for average inflation pressure and front-to-rear pressure differential according to vehicle age, size, and type are shown in Tables D.1a-c and Tables D.2a-c, respectively. In no case do these distributions depend on vehicle age or size. The influence of vehicle type was examined only for full-size cars because too few station wagons of intermediate size or smaller were contained in the sample. A significant difference in average inflation pressure between wagons and non-wagons appeared for 3-4-year-old vehicles. Also, a significant difference in inflation pressure differential between wagons and non-wagons showed up for 4-5-year-old vehicles. However, in the light of the similarity of these distributions for the other age groups and the small numbers of station wagons involved, these results were considered spurious. It was concluded that average inflation pressure and inflation pressure differential are not dependent on vehicle age, size, or type.

Table D.1a. Sample Sizes, Means, and Standard Deviations for Average Inflation Pressure by Vehicle Age and Size for Non-Station Wagons.

	Vehicle Age (yrs.)				
	0 - 1	1 - 2	2 - 3	3 - 4	4 - 5
Full	n = 16	32	39	58	62
	$\bar{x}$ = 25.4 psi	25.4	25.9	25.3	25.6
	s = 2.3 psi	2.8	2.7	2.9	3.4
Intermediate	30	36	40	41	41
	25.4	25.9	26.2	25.4	25.6
	3.6	3.5	2.9	2.5	2.7
Compact	12	17	27	31	18
	25.5	24.4	24.7	25.7	25.0
	2.7	3.2	3.0	2.8	3.0
Subcompact/ Mini	10	12	26	18	5
	25.8	25.4	24.6	24.6	23.8
	3.2	3.8	3.3	5.1	3.6

Table D.1b. Sample Sizes, Means, and Standard Deviations for Average Inflation Pressure by Vehicle Age and Size for Station Wagons.

		Vehicle Age (yrs.)			
	0 - 1	1 - 2	2 - 3	3 - 4	4 - 5
Full	n = 5	7	7	8	14
	$\bar{x}$ = 26.2 psi	25.1	25.1	27.1	26.3
	s = 3.0 psi	2.7	3.8	1.6	3.9
Intermediate	1	0	1	3	2
	21.0		29.0	27.3	26.0
				0.58	1.4

Table D.1c. Sample Sizes, Means, and Standard Deviations for Average Inflation Pressure by Vehicle Age and Type for Full-Size Vehicles.

		Vehicle Age (yrs)			
	0 - 1	1 - 2	2 - 3	3 - 4	4 - 5
Non-Wagon	n = 16	32	39	58	62
	$\bar{x}$ = 25.4 psi	25.4	25.9	25.3	25.6
	s = 2.3 psi	2.8	2.7	2.9	3.4
Wagon	5	7	7	8	14
	26.2	25.1	25.1	27.1	26.3
	3.0	2.7	3.8	1.6	3.9

Table D.2a. Sample Sizes, Means, and Standard Deviations for Inflation Pressure Differential by Vehicle Age and Size for Non-Station Wagons.

		Vehicle Age (yrs)				
		0 - 1	1 - 2	2 - 3	3 - 4	4 - 5
Full	n =	16	36	39	58	62
	$\bar{x}$ =	0.31 psi	0.06	0.36	0.76	0.40
	s =	1.25 psi	1.01	1.53	1.39	1.56
Intermediate		30	36	40	41	41
		0.40	0.39	0.58	0.34	0.24
		1.48	1.71	1.66	1.77	2.00
Compact		12	17	27	31	18
		0.42	0	0.37	0.10	0
		1.08	1.37	1.01	2.02	1.28
Subcompact/ Mini		10	12	26	18	5
		-0.40	1.00	1.08	-0.28	1.60
		1.17	2.09	2.59	1.81	3.58

Table D.2b. Sample Sizes, Means, and Standard Deviations for Inflation Pressure Differential by Vehicle Age and Size for Station Wagons.

	Vehicle Age (yrs)				
	0 - 1	1 - 2	2 - 3	3 - 4	4 - 5
Full	n = 5	7	7	8	14
	$\bar{x}$ = -0.20 psi	0	- 0.14	0	-1.14
	s = 1.30 psi	1.53	1.46	1.41	1.46
Intermediate	1	0	1	3	2
	-2.00		1.00	-0.67	-1.50
				1.15	2.12

Table D.2c. Sample Sizes, Means, and Standard Deviations for Inflation Pressure Differential by Vehicle Age and Type for Full-Size Vehicles.

	Vehicle Age (yrs)				
	0 - 1	1 - 2	2 - 3	3 - 4	4 - 5
Non-Wagon	n = 16	36	39	58	62
	$\bar{x}$ = 0.31 psi	0.06	0.36	0.76	0.40
	s = 1.25 psi	1.01	1.53	1.39	1.56
Wagon	5	7	7	8	14
	-0.20	0	-0.14	0	-1.14
	1.30	1.53	1.46	1.41	1.46

Statistics for average tread depth and front-to-rear tread depth differential are shown in Tables D.3a-c and D.4a-c, respectively. Some dependencies were discovered for these variables, and the cases for which significant differences were found are listed below:

Average Tread Depth:

- vehicle age influential for non-wagons for all vehicle sizes
- vehicle size influential for non-wagons (age groups 1-2, 3-4, and 4-5 years)

Tread Depth Differential:

- vehicle age influential for non-wagons in subcompact/mini category only
- vehicle size influential for non-wagons (4-5 year old vehicles only)

Age did not have a statistically significant influence for either variable for station wagons, nor did vehicle type have an effect on either variable.

The above analysis indicates that vehicle age has an influence on the distribution of average tread depth. Indeed, newer vehicles had substantially more tread than older vehicles, a finding that is to be expected. The data also indicated that vehicle size has some influence on average tread depth. This result appears to be caused by tread depths which are somewhat lower for vehicles in the subcompact/mini category than for other size vehicles.

As a result of the above findings, it was concluded that the checklane data on pressure and tread depths should be divided into five categories, one for each age group. Further sub-dividing according to size was excluded for the following reasons: (1) the influence of vehicle size on average tread depth is somewhat less

Table D.3a. Sample Sizes, Means, and Standard Deviations for Average Tread Depth by Vehicle Age and Size for Non-Station Wagons.

		Vehicle Age (yrs)				
		0 - 1	1 - 2	2 - 3	3 - 4	4 - 5
Full	n =	19	35	52	74	78
	$\bar{x}$ =	10.05 (1/32")	8.23	7.44	8.00	7.46
	s =	0.97 (1/32")	1.44	1.92	1.90	1.93
Intermediate		32	41	44	48	45
		9.66	8.44	7.70	7.15	7.27
		1.10	1.29	1.85	2.25	2.04
Compact		13	18	34	35	20
		9.54	8.17	7.24	7.31	6.60
		1.05	1.50	2.18	2.53	2.60
Sub-Compact/ Mini		11	15	26	22	7
		9.09	6.93	6.96	6.27	4.71
		0.94	2.37	1.93	1.45	1.70

Table D.3b. Sample Sizes, Means, and Standard Deviations for Average Tread Depth by Vehicle Age and Size for Station Wagons.

		Vehicle Age (yrs)			
	0 - 1	1 - 2	2 - 3	3 - 4	4 - 5
Full	n = 5	7	7	10	13
	$\bar{x}$ = 11.00 (1/32")	8.43	7.86	8.70	9.15
	s = 1.00 (1/32")	1.81	2.48	1.49	2.70
Intermediate	1	0	3	3	3
	10.0		7.67	7.67	8.33
			1.53	1.53	2.08

Table D.3c. Sample Sizes, Means, and Standard Deviations for Average Tread Depth by Vehicle Age and Type for Full-Size Vehicles.

		Vehicle Age (yrs)			
	0 - 1	1 - 2	2 - 3	3 - 4	4 - 5
Non-Wagon	n = 19	35	52	74	78
	$\bar{x}$ = 10.05 (1/32")	8.23	7.44	8.00	7.46
	s = 0.97 (1/32")	1.44	1.92	1.90	1.93
Wagon	5	7	7	10	13
	11.00	8.43	7.86	8.70	9.15
	1.00	1.81	2.48	1.49	2.70

Table D.4a. Sample Sizes, Means, and Standard Deviations for Tread Depth Differential by Vehicle Age and Size for Non-Station Wagons.

		Vehicle Age (yrs)				
		0 - 1	1 - 2	2 - 3	3 - 4	4 - 5
Full	n =	19	35	52	74	78
	$\bar{x}$ = (1/32")	0.00	-0.09	0.63	0.36	0.36
	s = (1/32")	0.47	0.70	1.28	1.35	1.38
Intermediate		32	41	44	48	45
		0.22	-0.12	0.16	0.23	0.36
		0.66	1.08	1.35	1.32	1.49
Compact		13	18	34	35	20
		0.31	0.50	0.09	0.23	-0.25
		0.63	1.38	1.36	1.11	1.52
Subcompact/ Mini		11	15	26	22	7
		0.36	0.07	-0.12	0.00	-1.14
		0.67	0.80	1.37	1.45	0.69

Table D.4b. Sample Sizes, Means, and Standard Deviations for Tread Depth Differential by Vehicle Age and Size for Station Wagons.

	Vehicle Age (yrs)				
	0 - 1	1 - 2	2 - 3	3 - 4	4 - 5
Full	n = 5	7	7	10	13
	$\bar{x}$ = 0.20 (1/32")	-0.43	-0.14	0.20	0.38
	s = 0.45 (1/32")	1.27	1.35	1.40	1.04
Intermediate	1	0	3	3	3
	0		0	0.67	0.67
			1.00	2.31	1.15

Table D.4c. Sample Sizes, Means, and Standard Deviations for Tread Depth Differential by Vehicle Age and Type for Full-Size Vehicles.

	Vehicle Age (yrs)				
	0 - 1	1 - 2	2 - 3	3 - 4	4 - 5
Non-Wagon	n = 19	35	52	74	78
	$\bar{x}$ = 0 (1/32")	-0.09	0.63	0.36	0.36
	s = 0.47 (1/32")	0.70	1.28	1.35	1.38
Wagon	5	7	7	10	13
	0.20	-0.43	-0.14	0.20	0.38
	0.45	1.27	1.35	1.40	1.09

than the influence of vehicle age, (2) sub-dividing both by size and year makes the size of some cells too small to yield meaningful calculations of understeer and steering sensitivity distributions, and (3) the extremely low value of average tread depth for the 1972 subcompact/mini category may be a spurious result because of the very small number of vehicles falling into that category. The numbers of vehicles in each age category are shown in Table D.5.

D.2 Distribution of Vehicle Loadings

Loads carried by passenger cars consist of occupants and cargo carried, if any. In this study, occupant loadings only were considered since data indicating the weight of cargo carried by in-use vehicles is not available. However, it is believed that most in-use passenger cars carry very little weight in their cargo area.

Data indicating the number of occupants typically carried in passenger cars was obtained from a study performed by the Federal Highway Administration [24]. These data produce the distribution reproduced in Table D.6. Unfortunately, this distribution (or probability) is not related to the number of occupants a particular car is designed to carry. Accordingly, separate distributions were derived from this overall distribution for cars with capacities of 2, 4, 5, and 6 persons. Distributions for vehicles capable of carrying more than 6 passengers were not developed since the incidence of cars that can carry more than 6 passengers, together with the probability of actually observing more than 6 passengers, are both small enough that it is believed that little error is incurred by ignoring such an occurrence. The distributions derived for cars of different seating capacity are presented in Tables D.7a-d. For purposes of calculation, a weight of 150 pounds per passenger was assumed.

Front- and rear-axle loads were computed for each passenger configuration by means of the front and rear seat occupant weight distributions given in the MVMA specification sheets. Since data are not available indicating where people tend to sit in cars, it

Table D.5. Numbers of Vehicles in Each Age Category.

Vehicle Age (Yrs.)	Number
0-1	74
1-2	104
2-3	141
3-4	159
4-5	140

Table D.6. Distribution of Number of Occupants.

Number of Occupants	Percentage
1	50.9
2	27.3
3	9.9
4	5.7
5	2.9
6	1.5
7	0.7
8	0.2
9 or more	0.3
N/A	0.6

was necessary to assume the order in which seats would be occupied as the number of occupants increases. In accounting for the influence of passenger loading, the first two occupants were placed in the front seat, the next three in the rear seat, and the sixth in the front seat. For vehicles with fewer than six seats, the order of seat occupancy was merely truncated at the appropriate seating capacity.

Table D.7. Occupant Distributions for Vehicles of Various Seating Capacities.

Occupants	Percentage
1	65.1
2	34.9

a) Two Occupant Vehicles

Occupants	Percentage
1	54.2
2	29.1
3	10.6
4	6.0

b) Four Occupant Vehicles

Occupants	Percentage
1	52.6
2	28.3
3	10.3
4	5.9
5	3.0

c) Five Occupant Vehicles

Occupants	Percentage
1	51.8
2	27.8
3	10.1
4	5.8
5	2.9
6	2.7

d) Six Occupant Vehicles

APPENDIX E

MAKE/MODEL DISTRIBUTION OF THE AT-RISK POPULATION

Clearly, it is not possible to identify with precision the at-risk population of cars that become involved in accidents in Oakland and Washtenaw Counties. For purposes of this study, the assumption was made that the at-risk population is defined by all of the domestic passenger vehicles registered in these two counties. Any local biases in the distribution of makes/models constituting the at-risk population would thus be taken into account.

To determine the vehicles registered in Oakland and Washtenaw Counties, magnetic tapes containing the desired registration data were obtained from the office of the Secretary of State of Michigan. These tapes contained a random sample of the vehicles registered, consisting of approximately ten percent (about 70,000) of the total. Information on the make/model and model year was deciphered from the VIN numbers with the aid of a computer program, VINDICATOR '77. Of the original 70,000 vehicles (approximately), 28,239 were identified as domestic passenger cars, model year 1972-1976. After aggregating the count by make, model, and model year, the number of vehicles registered for each make, model, and model year was added to file CARPARAM. With this information, it was possible to weight the in-use distributions of understeer and steering sensitivity computed for each make, model, and model year and thereby account for their presence in the total at-risk population.

APPENDIX F

DOCUMENTATION OF THE COMPUTATIONAL ALGORITHMS EMPLOYED

This appendix outlines, in detail, the procedures used to compute the understeer and steering sensitivity distributions for the OE, at-risk, and accident vehicle populations.

F.1 The OE Vehicle Population

A flow chart of the procedure used to calculate the distribution of understeer and steering sensitivity applicable to the OE vehicle population is shown in Figure F.1.

Three data files contain the required vehicle and tire information. File 'CARPARAM' contains data for each vehicle that was extracted from the MVMA specification sheets, e.g., weights, tire size, spring rates, etc. File 'DATA1' contains descriptors for each tire tested by Calspan. File 'DATA2' contains stiffnesses measured by Calspan for each tire contained in file 'DATA1'.

To begin the procedure, the program PREPTAXIR reads the tire size and rim diameter for each vehicle from CARPARAM and forms statements known as QUERY statements for processing by *TAXIR. These QUERY statements, one for each vehicle, are placed in file TAXIRINPUT. The QUERY statements contain tire size, rim diameter, and carcass type in a format acceptable to *TAXIR.

The program *TAXIR reads a QUERY statement from TAXIRINPUT and returns tire identification numbers from file DATA1 for all tires matching the descriptors in that QUERY statement. All the QUERY statements are processed in this manner. Thus, *TAXIR produces a list of tire identification numbers for each vehicle, and puts these into file TAXIROUTPUT. Because file TAXIROUTPUT contains some extraneous material, it is edited by program TXROUTFIX, and the edited contents are placed in file PREPSTIFFSIN.

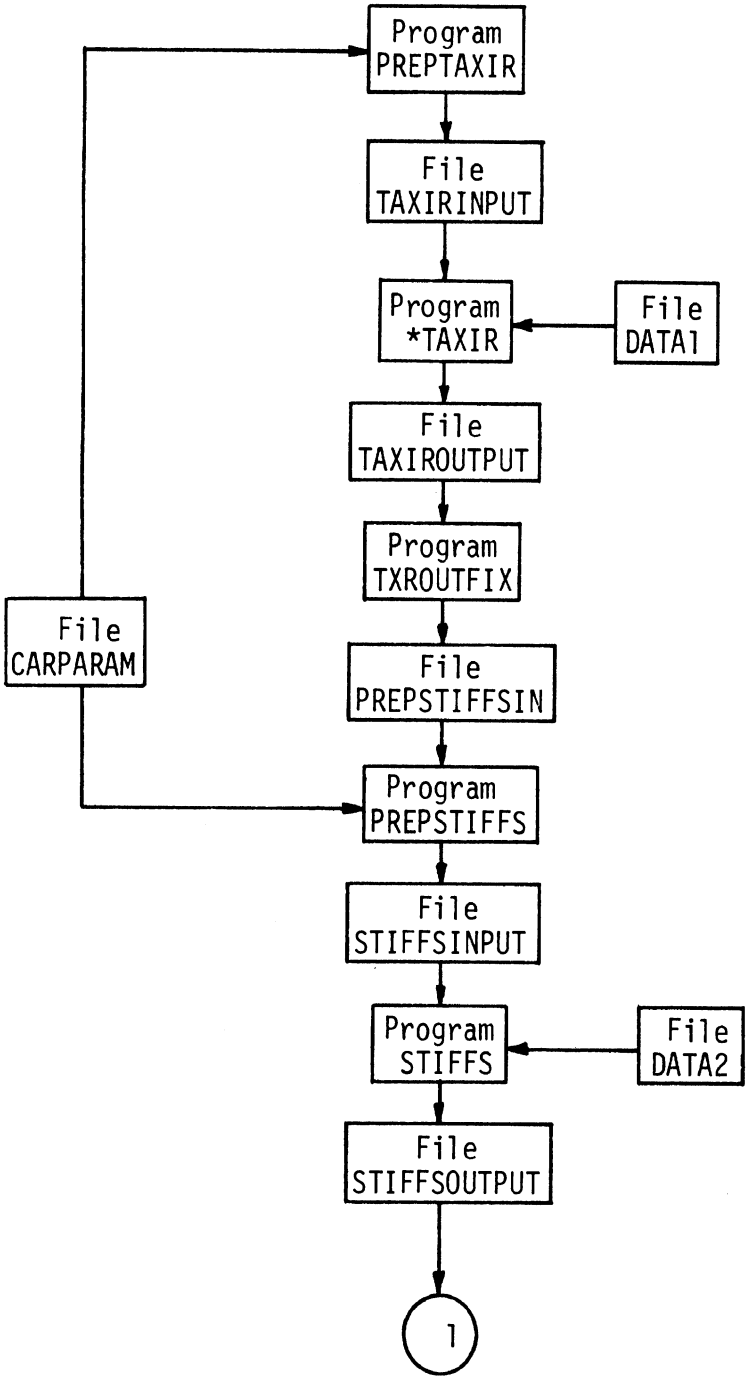

Figure F.1. Flow diagram of calculation of understeer/steering sensitivity distributions for the OE vehicle population.

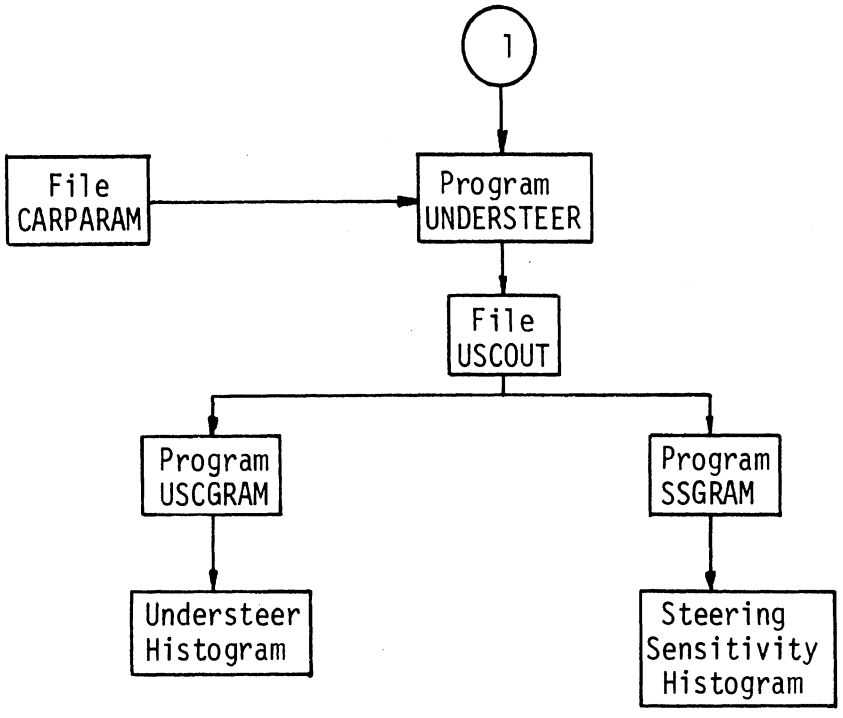

Figure F.1. (Cont.)

The next step in the processing involves program PREPSTIFFS which uses files PREPSTIFFSIN and CARPARAM as input. This program writes a file containing the information necessary to calculate the stiffnesses of the tires mounted on each vehicle. Front and rear axle loads are computed from information contained in CARPARAM, and front and rear inflation pressures are also read from the same file. This information is combined with the tire identification numbers in file PREPSTIFFSIN and placed in file STIFFSINPUT.

Program STIFFS reads the tire test data from file DATA2 and then reads the information for each vehicle from file STIFFSINPUT. Tire stiffnesses are calculated using the Calspan data and the inflation pressure correction outlined earlier. The resulting tire stiffnesses are put into file STIFFSOUTPUT.

Program UNDERSTEER reads tire stiffnesses from STIFFSOUTPUT and necessary vehicle data from CARPARAM and computes the understeer coefficient and steering sensitivity for each vehicle. The results of these computations are put into file USOUTPUT.

Finally, the understeer coefficients and steering sensitivities in file USOUTPUT are processed by programs USCGRAM and SSGRAM to produce histograms of these quantities.

F.2 The At-Risk Vehicle Population

A flow chart of the process used to calculate the distributions of understeer and steering sensitivity applicable to the at-risk vehicle population is shown in Figure F.2. The procedure is identical to that for the OE vehicle population up to the point of producing the file PREPSTIFFSIN.

At this point, program PREPSTIFFS2 reads the tire size for each vehicle from CARPARAM in order to provide information needed by the stiffness correction equations. This information is combined with the tire identification numbers from file PREPSTIFFSIN and written

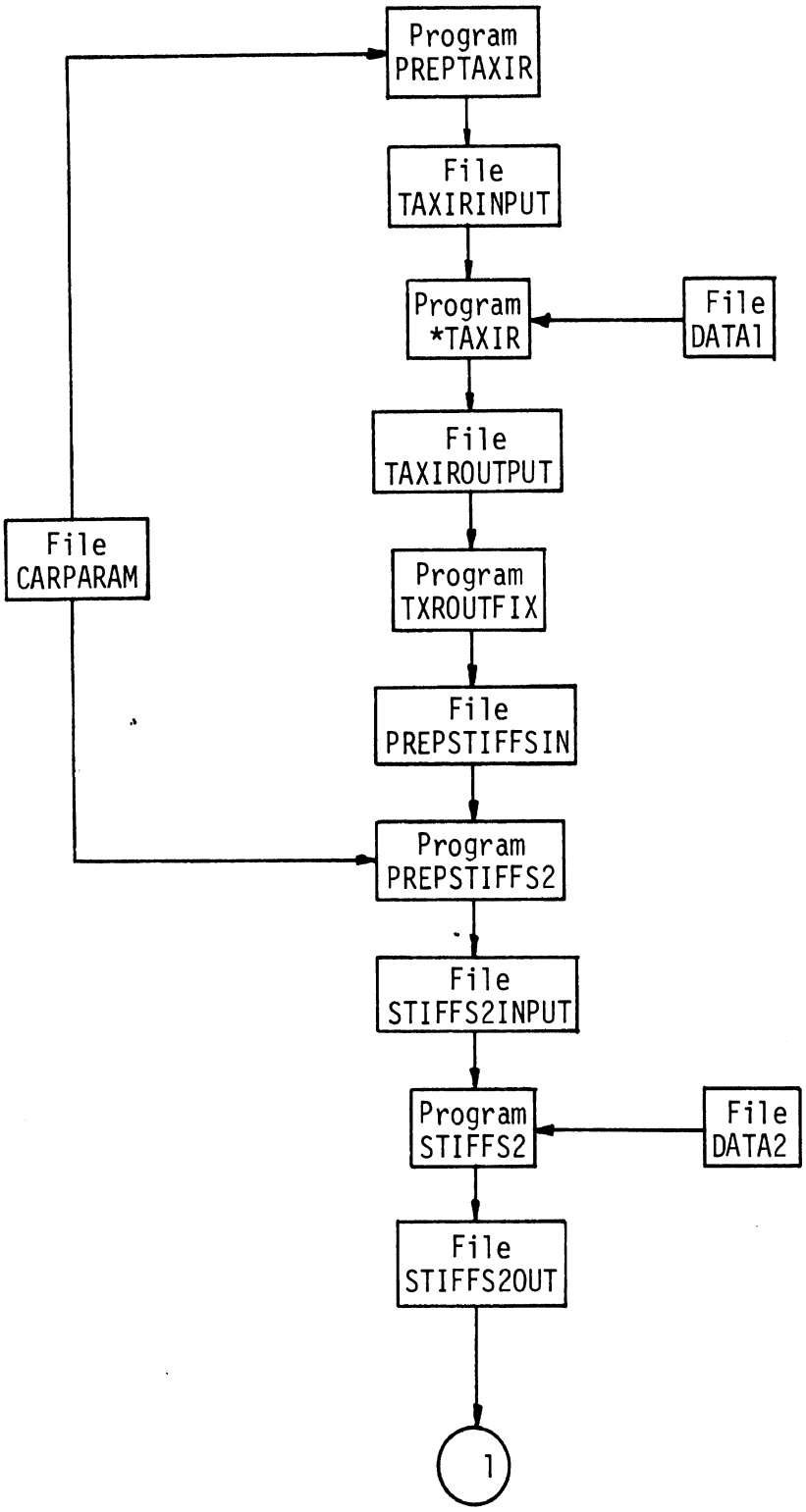

Figure F.2. Flow diagram of calculation of understeer/steering sensitivity distributions for the at-risk population.

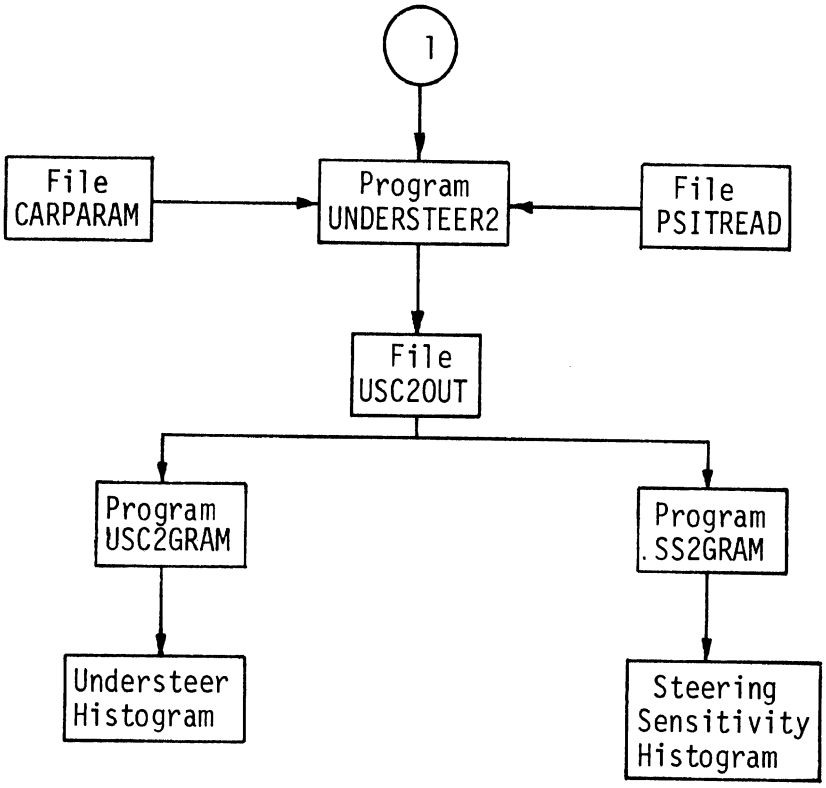

Figure F.2. (Cont.)

into file STIFFS2INPUT. Program STIFFS2 then makes some preliminary tire stiffness calculations. The tire stiffness data is read from file DATA2, and cornering and aligning stiffnesses at 24 psi and rated load are computed. Front and rear axle loads for each number of occupants that each vehicle is designed to carry are computed from information contained in CARPARAM. The camber stiffness of the front tire is then calculated for each loading condition and 24 psi. The resulting axle loads and tire stiffnesses are written into file STIFFS2OUT.

The next step in the processing is program UNDERSTEER2 which computes the distributions of understeer and steering sensitivity for the entire at-risk population. The program accepts the information in file STIFFS2OUT, necessary vehicle data and the registration information from file CARPARAM, and inflation pressures and tread depths from the checklane data which are contained in file PSITREAD. The resulting distributions are put into file US2OUT.

Lastly, programs USC2GRAM and SS2GRAM read file US2OUT to produce histograms of the in-use distributions of understeer and steering sensitivity.

F.3 The Accident Population

The computing algorithm for the accident population is very similar to that for the OE population. The differences are that tire stiffness calculations are made for all four tires on each vehicle and a new data file, ACC.CASES, containing the accident vehicle data, is used. A flow chart of the procedure is shown in Figure F.3.

To begin, program PREPTAXIR3 reads the four tire sizes for each vehicle from file ACC.CASES and prepares QUERY statements which are processed by *TAXIR. The resulting tire identification numbers are

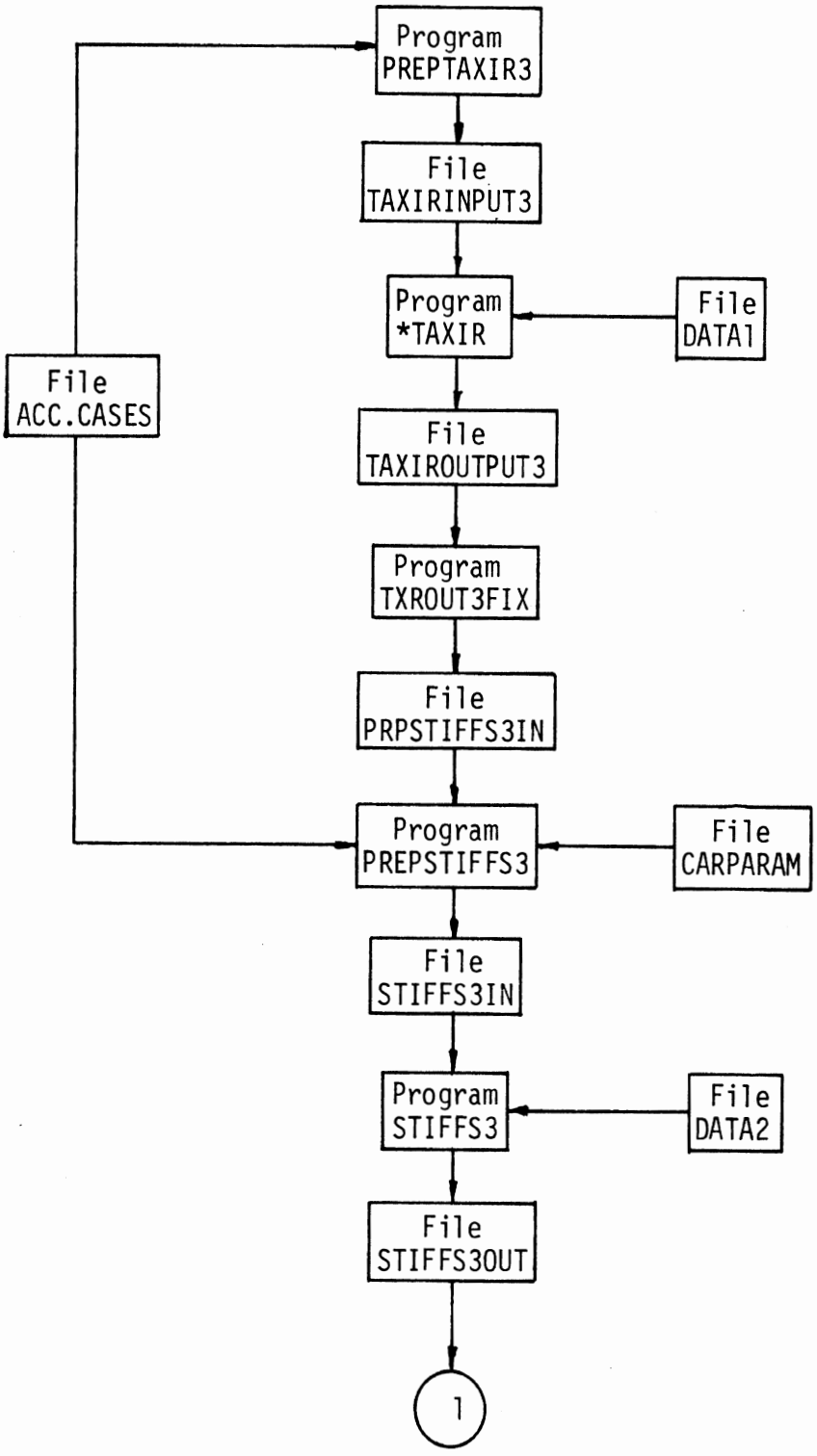

Figure 3. Flow diagram of calculation of understeer/steering sensitivity distributions for the accident population.

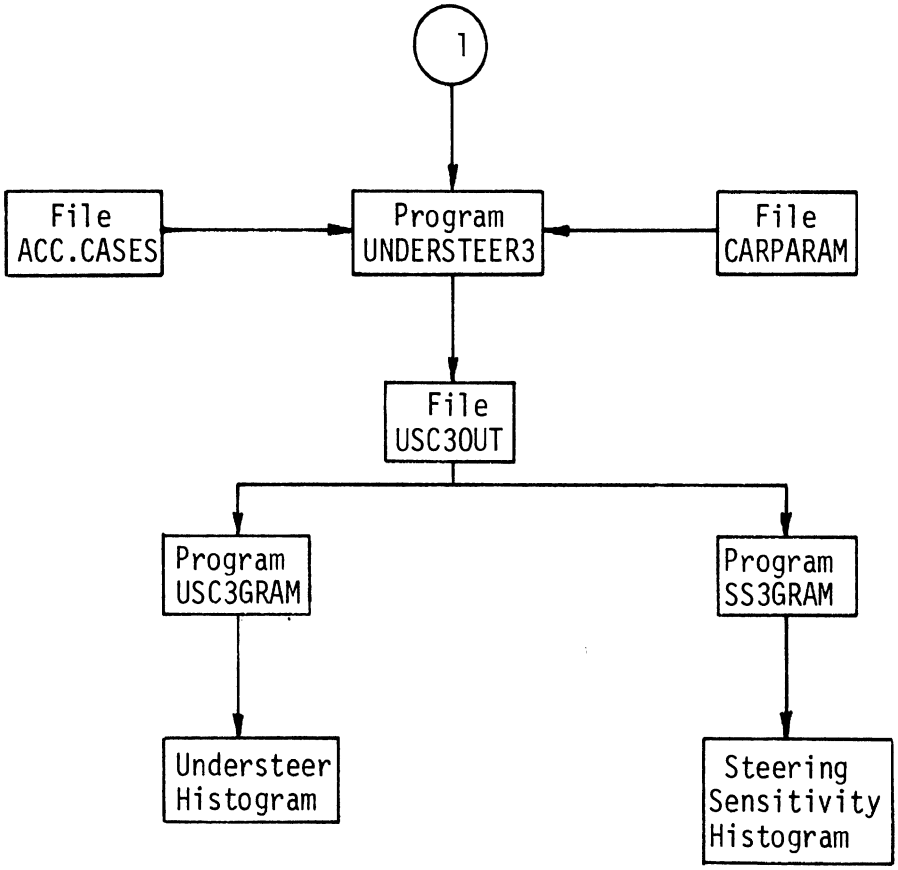

Figure F.3. (Cont.)

placed into file TAXIROUTPUT3. This file is edited by program TXROUT3FIX and the edited contents placed into file PRPSTIFF3IN.

Program PREPSTIFFS3 prepares input for program STIFFS3. The tire identification numbers are read from file PRPSTIFFS3IN and combined with tire size, inflation pressure, and tread depth information from file ACC.CASES and axle loads calculated from information contained in file CARPARAM and file ACC.CASES. All of this information is written into file STIFFS3IN.

Program STIFFS3 calculates cornering stiffnesses for all four tires and aligning and camber stiffnesses for the front tires and puts this information into file STIFFS3OUT. The stiffnesses are calculated from the data contained in file DATA2 and corrected for inflation pressure and tread depth.

With the tire stiffnesses available in file STIFFS3OUT, understeer coefficients and steering sensitivities are then calculated for each accident vehicle by program UNDERSTEER3. Necessary vehicle parameters are obtained from file CARPARAM and occupant weights from file ACC.CASES. The understeer coefficient and steering sensitivity for each vehicle is placed in file USC3OUT.

Finally, histograms of the understeer coefficients and steering sensitivities are produced with the aid of programs USC3GRAM and SS3GRAM.

REFERENCES

1. Dunlap, D.F., Segel, L., Preston, F.L., Cooley, P., and Brown, B.C. A Methodology for Determining the Role of Vehicle Handling in Accident Causation. Final Report, DOT/HS 802 261. Ann Arbor, Mi.: Highway Safety Research Institute, University of Michigan, February 1977.

2. Bundorf, R.T. "The Influence of Vehicle Design Parameters on Characteristic Speed and Understeer." SAE Paper No. 670078, 1967.

3. Bergman, W. "The Basic Nature of Vehicle Understeer-Oversteer." SAE Paper No. 957B, 1965.

4. Pacejka, H.B. "Simplified Analysis of Steady-State Turning Behavior of Motor Vehicles. Part III: More Elaborate Systems." Vehicle System Dynamics, 2(4): 185-204, December 1973.

5. Schuring, D.J. Tire Parameter Determination. Final Report, DOT/HS 802 087, Buffalo, NY: Calspan Corp., November 1976.

6. Bernard, J.E., Fancher, P.S., Gupta, R., Moncarz, H., and Segel, L. Vehicle-In-Use Limit Performance and Tire Factors - The Tire In Use. Final Technical Report, DOT/HS 801 439, Ann Arbor, Mi.: Highway Safety Research Institute, University of Michigan, January 1975.

7. Johnston, D.E., Zellner, J.W., and Ashkenas, I.L. Handling Test Procedures for Passenger Cars Pulling Trailers. Volume II: Technical Report, DOT/HS 801 936, Hawthorne, CA: Systems Technology, Inc., June 1976.

8. Vehicle Handling. Volume II: Technical Report, Report No. 5152, Southfield, Mi.: Bendix Research Laboratories, April 1970.

9. Vehicle Handling: A Simulation Study of the Handling Performance of Thirteen Configurations of an Intermediate Size American Passenger Car. Contract No. FH-11-7571, Southfield, Mi.: Bendix Research Laboratories, November 1970.

10. Tishkowski, J.R. [Letter to members of SAE Vehicle Dynamics Committee concerning proposed Standard XJ266 entitled, "Passenger Car and Light Truck Steady-State Directional Control Response Test Procedures"]. February 16, 1976.

11. Evaluation of the Michigan Checklane System. Highway Safety Research Institute, University of Michigan, Agreement N-2 of June 6, 1975; sponsoring agency: Michigan State Police.

12. Ward's Automotive Yearbook (for years 1973-1977). Detroit, Mi.: Ward's Communications, Inc., 1973-1977.

13. Oakland County Collision Investigation Project. Highway Safety Research Institute, University of Michigan, Project No. 4.10; sponsoring agency: MVMA.

14. Washtenaw County Collision Investigation Project. Highway Safety Research Institute, University of Michigan, Project No. 4.24; sponsoring agency: MVMA.

15. Wild, R.E., Young, R.D., MacAdam, C.C., and Gupta, R. Vehicle-In-Use Limit Performance and Tire Factors - The Tire In Use. Appendices D, E, F, G. Final Report, DOT/HS 801 437, Ann Arbor, Mi.: Highway Safety Research Institute, University of Michigan, January 1975.

16. Fancher, P.S., Ervin, R.D., Grote, P., MacAdam, C.C. and Segel, L. Limit Handling Performance as Influenced by Degradation of Steering and Suspension Systems. Final Report, DOT/HS 800 761, Ann Arbor, Mi.: Highway Safety Research Institute, University of Michigan, November 1972.

17. Schuring, D.J., Kunkel, D.T, Massing, D.E., and Roland, R.D. The Influence of Tire Properties on Passenger Vehicle Handling. Volume III: Appendices A-E. Final Report, DOT/HS 801 325, Buffalo, NY: Calspan Corp., June 1974.

18. Basso, G.L. Functional Derivation of Vehicle Parameters for Dynamic Studies. Ottawa, Ontario (Canada): National Research Council, National Aeronautical Establishment, LTR-ST.747, September 1974.

19. Computer Simulation of Vehicle Handling. Final Report DOT/HS 800 789, Southfield, Mi.: Bendix Research Laboratories, September 1972.

20. Weir, D.H., Hoh, R.H., Heffley, R.K., and Teper, G.L. An Experimental and Analytical Investigation of the Effect of Bus-Induced Aerodynamic Disturbances on Adjacent Vehicle Control and Performance. STI TR-1016-1, Hawthorne, CA: Systems Technology, Inc., November 1972.

21. Bohn, P.F., and Keenan, R.J. Hybrid Computer Vehicle Handling Program. Silver Springs, MD: Applied Physics Laboratory, Johns Hopkins University, Final Report, DOT/HS 801 290, November 1974.

22. Vindicator 77 Users' Guide: Release No. 2. Washington, D.C., Highway Loss Data Institute, April 1977.

23. Freund, J.E. Modern Elementary Statistics. Englewood Cliffs, NJ: Prentice-Hall, Inc., 1967.

24. Strate, H.E. Nationwide Personal Transportation Survey: Automobile Occupancy. Washington, D.C.: Federal Highway Administration, April 1972.